Adolescent alcohol consumption alters sex-specific behaviors associated with prefrontal functional connectivity in mice

Running title: adolescent alcohol behavior and imaging

Laurel R. Seemiller[1,2,3], Hayreddin Said Ünsal[4,5], Yiyan Xie[1,2,4], Md Shakhawat Hossain[2,3,6], Kaleah Tuttle[1], Bryce Johnson-Dendy[1], Emily P. McDonald[1], Patrick J. Drew[1,2,3,4,6,7], Nanyin Zhang[2,3,4], and Nicole A. Crowley[1,2,3,4,7]

[1] Department of Biology, The Pennsylvania State University, University Park, PA, 16802, USA

[2] Penn State Neuroscience Institute, The Huck Institutes of the Life Sciences, University Park, PA, 16802, USA

[3] Center for Neural Engineering, The Pennsylvania State University, University Park, PA, 16802, USA

[4] Department of Biomedical Engineering, The Pennsylvania State University, University Park, PA, 16802, USA

[5] Department of Electrical and Electronics Engineering, Abdullah Gül University, Kayseri, Türkiye

[6] Department of Engineering Science and Mechanics, The Pennsylvania State University, University Park, PA, 16802, USA

[7] Department Neurosurgery, The Pennsylvania State University, University Park, PA, 16802, USA

Corresponding Author Contact:

Nicole A. Crowley, Ph.D.

W309 Millennium Science Complex

Penn State University

University Park, PA, USA 16802

nzc27@psu.edu

ABSTRACT

The prefrontal cortex (PFC) is one of the last brain regions to fully mature, making it particularly sensitive to drug use early in life. Both human and rodent studies find long-lasting behavioral changes after adolescent alcohol exposure that implicate underlying disruptions in PFC development, including structural abnormalities and altered brain functional connectivity. Few rodent studies have been conducted to understand the network-level implications of these disruptions. We assessed how adolescent binge-like alcohol consumption in a drinking in the dark (DID) model affected adult alcohol consumption, behavioral exploration, and brain-wide functional connectivity in mice. Approximately one month after the conclusion of DID, only female mice exposed to alcohol during adolescence exhibited aversion-resistant alcohol preference in adulthood. Adult females exhibited additional sex-specific changes in exploratory behavior in the elevated plus maze after adolescent alcohol consumption. Resting state neuroimaging revealed sex-specific changes in prefrontal cortical connections with sensory motor, hippocampal, striatal, and other networks, providing insights into the putative systems underlying deficits caused by adolescent alcohol exposure. Critically, our data corroborate a growing body of literature in human and rodent studies demonstrating that adolescent alcohol use may increase risk for adult alcohol use more strongly in females. Finally, we identify neural correlates of this effect that include both known and novel neural networks and tie these back to human datasets, allowing biological and mechanistic targets to be further explored for future study and interventions.

KEYWORDS: adolescent, alcohol, DID, prefrontal, aversion-resistant drinking, functional connectivity, fMRI

1. INTRODUCTION

Adolescent alcohol use is associated with increased adult alcohol use and increased risk of developing an alcohol-related disorder[1–3]. Recent data indicate that this risk persists throughout the lifetime, and these positive associations between adolescent and later life alcohol use are stronger in females than in males[3]. These and other lasting behavioral consequences of adolescent alcohol exposure are thought to be driven by disturbances in the natural development of both morphological characteristics and functional wiring properties of the brain. Normative adolescent brain development requires selective pruning of neuronal connections and cortical thinning[4], but adolescent alcohol use has been shown to disrupt rates of cortical thinning[5]. Complementary lines of evidence show disruptions in functional connectivity between the default-mode network and an intrinsic functional network implicated in regulating emotional responses[6] as well as within cortical and striatal networks[7], suggesting a potential network mechanism for the increased vulnerability seen to adult alcohol use disorder (AUD). Vulnerability to development of AUD can also be exacerbated by other psychiatric conditions, such as anxiety[8], which is heightened after alcohol use[9], suggesting reciprocal feedback between substance use and mood disorders[10].

Despite the known behavioral consequences of adolescent binge drinking and novel insights into brain connectivity changes made via functional imaging, further work must be done to bridge the gap between human epidemiological studies and the controlled assessment of the relationship between total alcohol intake and behavioral and mechanistic biological brain changes conducted with rodent studies. Here, we aimed to narrow this divide by examining the long-term consequences of voluntary alcohol consumption during adolescence in a mouse model. Male and female C57BL/6J mice received intermittent access to alcohol in a Drinking in the Dark (DID) paradigm[11] throughout adolescence and were tested for changes in aversion-resistant alcohol preference, exploratory behaviors, and whole-brain resting state functional connectivity[12] in adulthood. We found binge drinking-induced changes in alcohol preference, behaviors related to exploratory and anxiety phenotypes, and functional connectivity within a prefrontal polymodal association network, all of which showed marked sex differences. This data suggests alterations in prefrontal cortical networks induced by voluntary alcohol consumption may underlie adulthood shifts in risk-taking and executive-decision making behaviors, consistent with what has been proposed in the human literature[13]. Our current work further bridges the gap between human

epidemiological and behavioral studies and preclinical mechanistic biological studies via a shared non-invasive imaging dataset and allows for synthesis across human and animal studies.

2. MATERIALS AND METHODS

2.1 Animals

Male and female C57BL/6J (JAX #000664) mice were bred in-house for experiments beginning during adolescence (Bar Harbor, ME, USA; see **Supplemental Materials** for adult experiments). On postnatal day (PND) 21, mice were weaned and single-housed in a room with a reversed light cycle (lights off at 7:00 AM). They acclimated to these conditions for at least one week prior to experiments. Mice had ad libitum access to water and food outside of DID testing (LabDiet 5053, Lab Diet, St. Louis, MO, USA). During DID (described below), water bottles were replaced with alcohol bottles for 2-4 hr. All procedures were conducted in accordance with the NIH Guide for the Care and Use of Laboratory Animals and were approved by the Penn State Institutional Animal Care and Use Committee.

2.2 Drinking in the Dark (DID)

DID was performed as described previously as a method for producing robust binge-like alcohol consumption and blood ethanol concentrations above thresholds for intoxication[11,14–16]. Beginning on PND 29 (+/-1 day) for adolescent experiments, mice had intermittent access to 20% v/v ethanol (EtOH; Koptec, Decon Labs, King of Prussia, PA) in H2O (tap water). EtOH access began 3 hr into the dark cycle. For the first 3 days, alcohol access lasted 2 hr, and on the fourth day, alcohol access lasted 4 hr. After 3 days of abstinence, the DID cycle was repeated for a total of 4 cycles, with the last binge day falling on PND 53 (+/-1 day). Ages differed for additional adult behavioral experiments (see **Supplemental Materials**). Control subjects received access to water. Mice were weighed once weekly.

2.3 Preference for quinine-adulterated EtOH

Adulthood EtOH preference was measured as published previously[16,17]. On PND 77-80, mice began acclimation to sipper tubes containing H2O (tap water). Sipper tubes were weighed and refilled every 48-72 hr

to monitor intake. Approximately 30+ days after DID (PND 84-87) mice underwent a continuous access two-bottle choice paradigm (2BC) where they received access to one tube of H2O and one tube of increasing concentrations of EtOH in H2O (3% w/v EtOH for 2 days, 7% w/v EtOH for 5 days, and 10% w/v EtOH for two weeks) which we have shown to reliably produce EtOH preference[16,17]. After this acclimation procedure, the 10% w/v EtOH in tap water was mixed with increasing concentrations of quinine hydrochloride (0.03, 0.1, 0.3, and 1 mM). Positions of H2O and EtOH tubes were alternated after every refill to avoid side preferences. Preference for EtOH solutions was defined as (EtOH consumed / total fluid consumed). Mice were weighed once weekly.

2.4 Open field testing (OFT) and elevated plus maze (EPM)

Behaviors in the open field test (OFT) and elevated plus maze (EPM) were assessed roughly 30 days (or 24 hr, see **Supplemental Materials**) after DID during the dark stage of the light cycle and under red light (8:00 AM - 4:00 PM). Mice were transferred to a procedure room and acclimated for one hr prior to behavior testing. First, mice were placed in the corner of an open field box (50 × 50 cm; walls were 20 cm black plexiglass) and allowed to explore for 5 min[18–20]. After OFT testing, mice were returned to home cages in the procedure room and allowed to acclimate again for at least one hour before EPM testing. Then, mice were placed in the center of an elevated plus maze (30 × 5 cm arms; walls were 20 cm clear plexiglass on closed arms; maze was elevated 40 cm) and allowed to explore for 5 min[18]. EPM data were excluded after mice occasionally fell off of the maze (three times for primary experiment 30 days after adolescent DID), which weakened statistical power and could have introduced selection bias. Behavior was video-recorded and analyzed using DeepLabCut[21] and MATLAB (see **Supplemental Materials**).

2.5 Functional magnetic resonance imaging (fMRI)

Beginning four days prior to imaging, mice were briefly anesthetized with 3% isoflurane, secured in a restrainer, allowed to awake from anesthesia, and were restrained for 15, 30, 45, and 60 min on acclimation days 1-4, respectively, while a soundtrack of fMRI noises was played. Mice were anesthetized again before being removed from the restrainer. On PND 83-88 (at least 30 days after DID), awake resting state imaging was performed using a 7T MRI system and Bruker Console (Billerica, MA) using Paravision 7.0.0. Each scan lasted 10 min and collected 400 volumes, with three scans per mouse. Framewise displacement (FD) was calculated to

quantify motion[22]: $FD = |\Delta x| + |\Delta y| + |\Delta z| + r * (|\Delta\alpha| + |\Delta\beta| + |\Delta\gamma|)$. Motion calculation and correction were performed using the Statistical Parametric Mapping (SPM12) package (http://www.fil.ion.ucl.ac.uk/spm/). A total of 62 regions of interest (ROIs) were defined based on definitions from the Allen Mouse Brain Atlas[23]. Resting state functional connectivity between brain regions was analyzed using an ROI-based approach specifically testing Pearson correlations between the average activity time course between each ROI pair. Functional connectivity matrices were calculated using Fisher's z-transformed Pearson's correlation coefficients within each mouse. Methodological details for fMRI can be found in **Supplemental Materials**.

2.6 Statistics

Behavioral analysis: Statistical analysis was performed in GraphPad Prism (version 10; La Jolla, CA, USA) and MATLAB (R2021a; The MathWorks Inc., Natick, MA, United States) and figures were made in GraphPad Prism. A significance threshold of $\alpha = 0.05$ was used for all analyses. Two- and three-way ANOVA were used, employing a mixed model for repeated measures. Sex and alcohol interactions were followed up with post-hoc t tests with a Bonferroni correction between alcohol and control groups within each sex (two total t tests per interaction). Additional generalized linear mixed-effects (GLME) modeling in alcohol-exposed mice explored the relationship between total alcohol consumption and adult outcomes using the fitglme toolbox in MATLAB and accounted for litter and behavioral cohort as random effects. The model was defined as: [outcome variable] ~ 1 + Sex*EtOH + (1|Litter) + (1|Cohort). The link function was identity or log for variables with normal and Poisson distributions, respectively. When sex and alcohol interactions were detected, they were followed up with post-hoc additional GLME models within each sex: [outcome variable] ~ 1 + EtOH + (1|Litter) + (1|Cohort). More statistical details including management of missing data points and non-significant results can be found in **Supplemental Materials**.

fMRI analysis: Statistical analysis was performed and figures were made in MATLAB version R2023b (The MathWorks Inc., Natick, MA, United States). Runs with over 10% of volumes discarded due to motion artifacts were excluded from final analysis. The effects of adolescent alcohol consumption, sex, and their interaction on functional connectivity were assessed using a linear mixed model, with subject as a random effect.

3. RESULTS

3.1 Adolescent binge drinking led to minor differences in sex-specific physiological growth

Adolescent male and female mice received intermittent access to alcohol in a DID paradigm across all experiments. Daily alcohol consumption was analyzed via two-way (sex, day) mixed model ANOVA and body weights were analyzed via three-way (treatment, sex, week) mixed model ANOVA. In the first experimental cohort (**Fig 1A**), adolescent females consumed more alcohol than adolescent males ($F_{1,19} = 10.2$, $p = 0.0048$; **Fig 1B**). An interaction between treatment and sex was detected for body weight ($F_{1,33} = 4.1$, $p = 0.0498$; **Fig 1C**), and post-hoc two-way ANOVA (treatment, week) within sexes revealed that alcohol-treated females weighed less than female water controls ($F_{1,18} = 4.5$, $p = 0.0476$) and alcohol exposure interacted with week ($F_{3,54} = 3.2$, $p = 0.0309$). No treatment effect was seen for male body weights. No differences were seen in alcohol consumption

and body weight in the second (**Fig 1D-F**) and third (**Fig 1 G-I**) experimental cohorts. Additional sex and week effects on body weights are further described in **Supplemental Materials**.

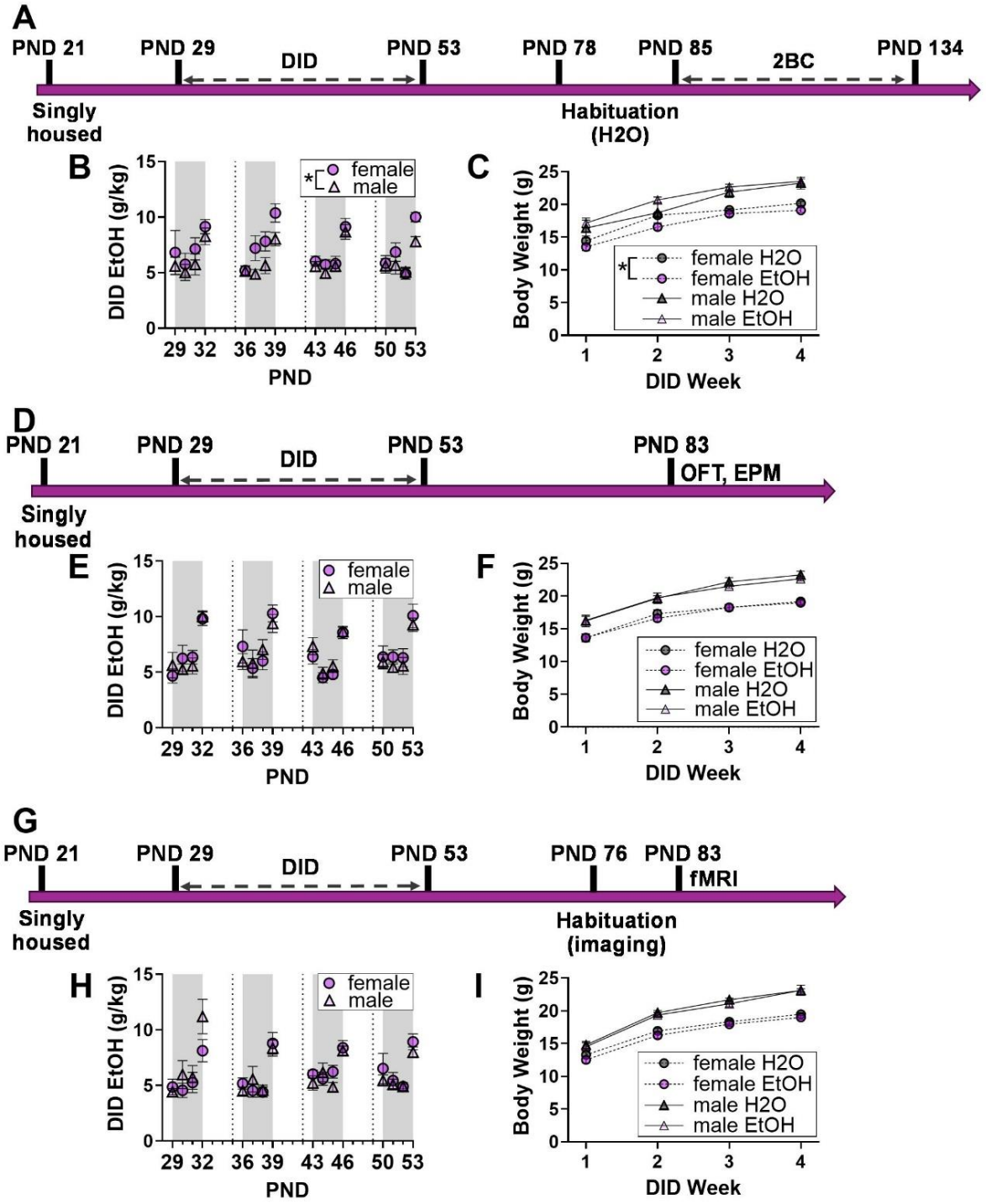

Figure 1: Experimental timelines, adolescent alcohol consumption, and body weights across cohorts. Three separate experiments tested the influence of adolescent drinking in the dark (DID) on adult aversion-resistant alcohol preference via two-bottle choice (2BC; **A-C**), exploratory behavior in the open field test (OFT) and elevated plus maze (EPM; (**D-F**), and whole brain resting state functional connectivity (**G-I**). PND is approximate (see methods). Data are shown as mean +/- SEM. *$p < 0.05$. n = 9-11 (**A-C**), 8-10 (**D-F**), or 11 (**G-I**) per sex per treatment.

3.2 Adult preference for alcohol and quinine-adulterated alcohol after adolescent drinking

Beginning approximately 30 days after adolescent drinking, adult mice received continuous access to a bottle of alcohol containing increasing concentrations of the bitter tastant quinine alongside a bottle of water (timeline in **Fig 1A**). Because adolescent females consumed more alcohol than adolescent males in this cohort, and because there were significant sex-dependent interactions between alcohol and physiological growth, adult males and females were analyzed separately for categorical (EtOH vs H2O groups) analyses. Preference, fluid consumption, and body weight were analyzed via two-way (treatment, week) mixed model ANOVA.

Adult females that consumed alcohol during adolescence exhibited stronger preference for alcohol and quinine-adulterated alcohol than females that only had water during adolescence ($F_{1,18} = 4.7$, $p = 0.0441$; **Fig 2A**). Female alcohol preference differences were likely driven by a reciprocal increase in alcohol and decrease in water consumption, as adult female alcohol, water, and total fluid consumption by themselves were not significantly altered by adolescent alcohol exposure (**Fig 2B-C, Supplemental Materials**). Adult female body weight was also not impacted by adolescent alcohol exposure, suggesting a recovery of their physiological growth trajectory (**Supplemental Materials**). In adult males, adolescent alcohol consumption did not significantly influence adult alcohol preference, alcohol consumption, water consumption, total fluid consumption, or body weight (**Fig D-F, Supplemental Materials**). Across females and males, all measures varied by week (F Pref: $F_{4,70} = 109.1$, $p < 0.0001$; F EtOH: $F_{5,81} = 99.42$, $p < 0.0001$; F H2O: $F_{4,75} = 124.5$, $p < 0.0001$; F Fluid: $F_{4,72} = 4.5$, $p = 0.0028$; F Weight: $F_{4,74} =$, $p < 0.0001$; M Pref: $F_{3,58} = 27.0$, $p < 0.0001$; M EtOH: $F_{3,58} = 43.7$, $p < 0.0001$; M H2O: $F_{4,68} = 39.9$, $p < 0.0001$; M Fluid: $F_{3,60} = 8.4$, $p < 0.0001$; M Weight: $F_{2,35} = 41.9$, $p < 0.0001$). Additional analyses showed that total adult alcohol consumed prior to alcohol was positively associated with total alcohol consumed with quinine (**Supplemental Materials**). Overall, adolescent alcohol consumption increased adult preference for alcohol and quinine-adulterated alcohol in females and not in males.

To directly compare sexes while accounting for differences in adolescent alcohol consumption, we used a GLME model. Before quinine was added to alcohol (weeks 2-4), average alcohol preference was inversely associated with total alcohol consumption (ado EtOH: -0.0092989 ± 0.0040242, $p = 0.0337$) and was lower in males than in females (quinine male: -1.22 ± 0.51557, $p = 0.0301$; **Fig 2G**). Similar effects of total adolescent alcohol and sex were seen on total adult alcohol consumption. Adolescent alcohol consumption was associated

with decreased adult alcohol consumption (ado EtOH: -77.03 ± 19.392, p = 0.0010) and males consumed less alcohol without quinine than females (male: -7300.1 ± 2334.3, p = 0.0061; **Fig 2H**). Total adult alcohol consumption without quinine was also influenced by an interaction of sex and adolescent alcohol (male x ado EtOH: 46.756 ± 21.202, p = 0.0415). Post-hoc analyses within sexes confirmed an effect of adolescent alcohol in males (ado EtOH: -20.486 ± 8.4987, p = 0.0392) but not in females. Adult total water consumption prior to quinine testing was not altered by sex or adolescent alcohol consumption (**Fig 2I**). In short, adolescent alcohol consumption was inversely associated with adult alcohol consumption and preference prior to quinine testing, and an interaction of adolescent alcohol with sex was noted for total quinine-free alcohol consumption.

Similar effects of total adolescent alcohol consumption and sex were seen on alcohol preference, alcohol consumption, and water consumption after quinine was included (weeks 5-8). Total adolescent alcohol consumption had an inverse association with average alcohol preference with quinine (ado EtOH: -0.010501 ± 0.0043085, p = 0.0261; **Fig 2J**), but sex effects on alcohol preference with quinine were not detected. Total adolescent alcohol consumption was associated with decreased adult alcohol consumption (ado EtOH: -85.924 ± 22.866, p = 0.0016) and adult males consumed less alcohol than adult females with quinine (male: -7122.3 ± 2759.8, p = 0.0194; **Fig 2K**). Further, during quinine testing, adolescent alcohol consumption was positively associated with adult water consumption (ado EtOH: 73.618 ± 23.207, p = 0.0056), adult males consumed more water than adult females (male: 6981.3 ± 3163.4, p = 0.0414), and sex and adolescent alcohol consumption interacted to influence adult water consumption (male x ado EtOH: -65.655 ± 29.139, p = 0.0377; **Fig 2L**). Post-hoc analyses within sexes found a significant positive effect of adolescent alcohol consumption on adult water consumption during quinine testing in females (ado EtOH: 73.618 ± 19.258, p = 0.0051) but not in males. Additionally, total fluid consumption and average body weight across all adult testing weeks were not impacted by sex or total adolescent alcohol consumption (**Supplemental Materials**). To summarize, total adolescent alcohol consumption had an inverse association with average adult preference and alcohol consumption during the quinine test (weeks 5-8). Overall changes in fluid consumption were not observed, suggesting a specific

effect of adolescent alcohol consumption on adult alcohol preference and not generalized consummatory behaviors.

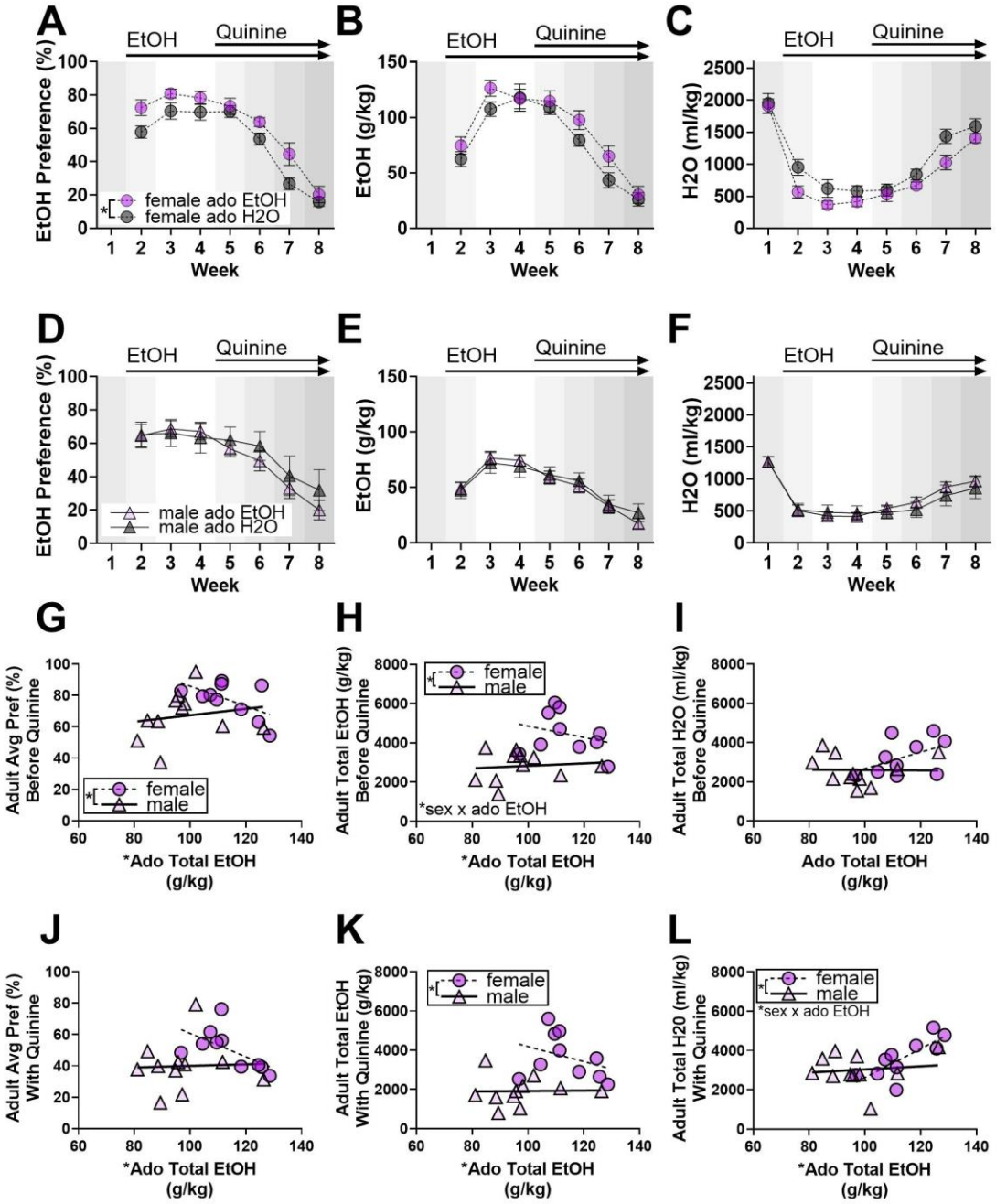

Figure 2: **Adolescent alcohol consumption increased adult preference for alcohol and quinine-adulterated alcohol in females and not in males. (A)** EtOH preference in females. **(B)** EtOH g/kg consumed by females. **(C)** Water consumed in ml/kg by females. **(D)** EtOH preference in males. **(E)** EtOH g/kg consumed by males. **(F)** Water consumed in ml/kg by males. **(G)** Average EtOH preference compared to adolescent EtOH consumption in females. **(H)** Total EtOH consumption during 2BC in g/kg compared to adolescent EtOH consumption by females. **(I)** Total water consumption during 2BC in ml/kg compared to adolescent EtOH consumption in females. **(J)** Average EtOH preference compared to adolescent EtOH consumption in males. **(K)** Total adult EtOH consumption during 2BC in g/kg compared to adolescent EtOH consumption in males. **(L)** Total water consumption during 2BC in ml/kg compared to adolescent EtOH consumption in males. Ado = Adolescent. Week 1 represents consumption of H2O only, Week 2 includes 3-7% EtOH, Week 3-4 represents 10% EtOH, and Weeks 5-8 represent 10% EtOH with increasing concentrations of quinine (0.03, 0.1, 0.3, and 1mM). Plots labeled as "Before Quinine" represent data from Weeks 1-4, and plots labeled as "With Quinine" represent data from Weeks 5-8. In scatter plots, a simple linear regression was used to generate lines of best fit and aid interpretation but were independent from statistical analysis. Data are shown as mean +/- SEM. * p <0.05. n=9-11/sex/treatment.

3.3 Adult exploration in the OFT and EPM after adolescent drinking

In a separate cohort of mice, approximately 30 days after adolescent drinking, we tested adult exploratory behaviors in the OFT and EPM (**Fig 1D**). Because adolescent mice of this cohort consumed comparable amounts of alcohol, males and females were includes in the same categorical (EtOH vs H2O groups) two-way (treatment, sex) ANOVA. Additional GLM analyses tested the relationship between total adolescent alcohol consumption and adult behavior among alcohol-exposed subjects.

First, mice were placed in an open field chamber and video recorded for 5 min. No effects of sex, adolescent alcohol treatment group, or total adolescent alcohol consumed were detected for OFT outcomes (**Fig 3A-F**). Next, following a recovery period in their home cage, mice underwent testing in the elevated plus maze and behavior was monitored over 5 min. Adolescent alcohol consumption and sex significantly interacted to alter latency to enter an open arm of the maze ($F_{1,32}$ = 4.4, p = 0.0446; **Fig 3G**), though post-hoc tests within sexes did not reveal differences across treatment groups. Time spent in open arms (**Fig 3H**) and number of open arm entries (**Fig 3I**) were not different across adolescent alcohol or sex groups. Additional analyses tested the associated between total adolescent alcohol consumption and adult behaviors in only alcohol-exposed mice, and no effects were seen for latency to enter EPM (**Fig 3J**), but this revealed an interaction of adolescent alcohol consumption and sex on time spent in the open arm (male x ado EtOH: 0.9827 ± 0.4244, p = 0.0363; **Fig 3K**) and open arm entries (male x ado EtOH: 1.0538 ± 0.4220, p = 0.0256; **Fig 3L**). Post-hoc analyses within sexes

revealed significant reductions in exploratory behaviors due to total alcohol exposure within females, and not males, as indicated by reduced time spent in the open arm (ado EtOH: -0.6544 ± 0.0290, $p < 0.0001$) and open arm entries (ado EtOH: -0.5535 ± 0.1947, $p = 0.0295$). Further, total adolescent alcohol consumption alone was significantly associated with latency to enter the open arm (ado EtOH: 0.0463 ± 0.01146, $p = 0.0011$). Sex was significantly associated with time spent in the open arms (male: -100.69 ± 45.956, $p = 0.0459$) and entries into open arms (male: -106.73 ± 45.694, $p = 0.0349$). Further, number of head dips (**Fig 3M**) and total distance traveled (**Fig 3N**) were not significantly affected by adolescent alcohol group or sex. In additional analyses testing effects of total alcohol consumed, a significant interaction of adolescent alcohol consumption and sex was detected for head dips (male x ado EtOH: 2.1466 ± 0.6536, $p = 0.0054$) in addition to a significant influence of total adolescent alcohol exposure (ado EtOH: -0.9572 ± 0.4410, $p = 0.0477$) and sex (male: -232.09 ± 70.78, $p = 0.0055$; **Fig 3O**). Post-hoc analyses within sexes showed significant reductions in head dips due to total alcohol exposure within females, and not males (ado EtOH: -1.0553 ± 0.2346, $p = 0.0041$). No effects of sex or total alcohol consumed were seen for distance traveled in the EPM (**Fig 3P**). In summary, across multiple measures, total adolescent alcohol consumption decreased EPM exploratory behaviors in females and not in males.

To understand whether the effects of alcohol were specific to adolescents or the 30-day post-DID timepoint, we investigated how the same DID paradigm affected adolescents 24 hr post-DID and adults 30 days post-DID (**Supplemental Materials**). There were only minor effects of alcohol on behavior in these experiments, suggesting that the adolescent period is uniquely vulnerable to alcohol and some behavioral effects of adolescent alcohol exposure may take time to emerge.

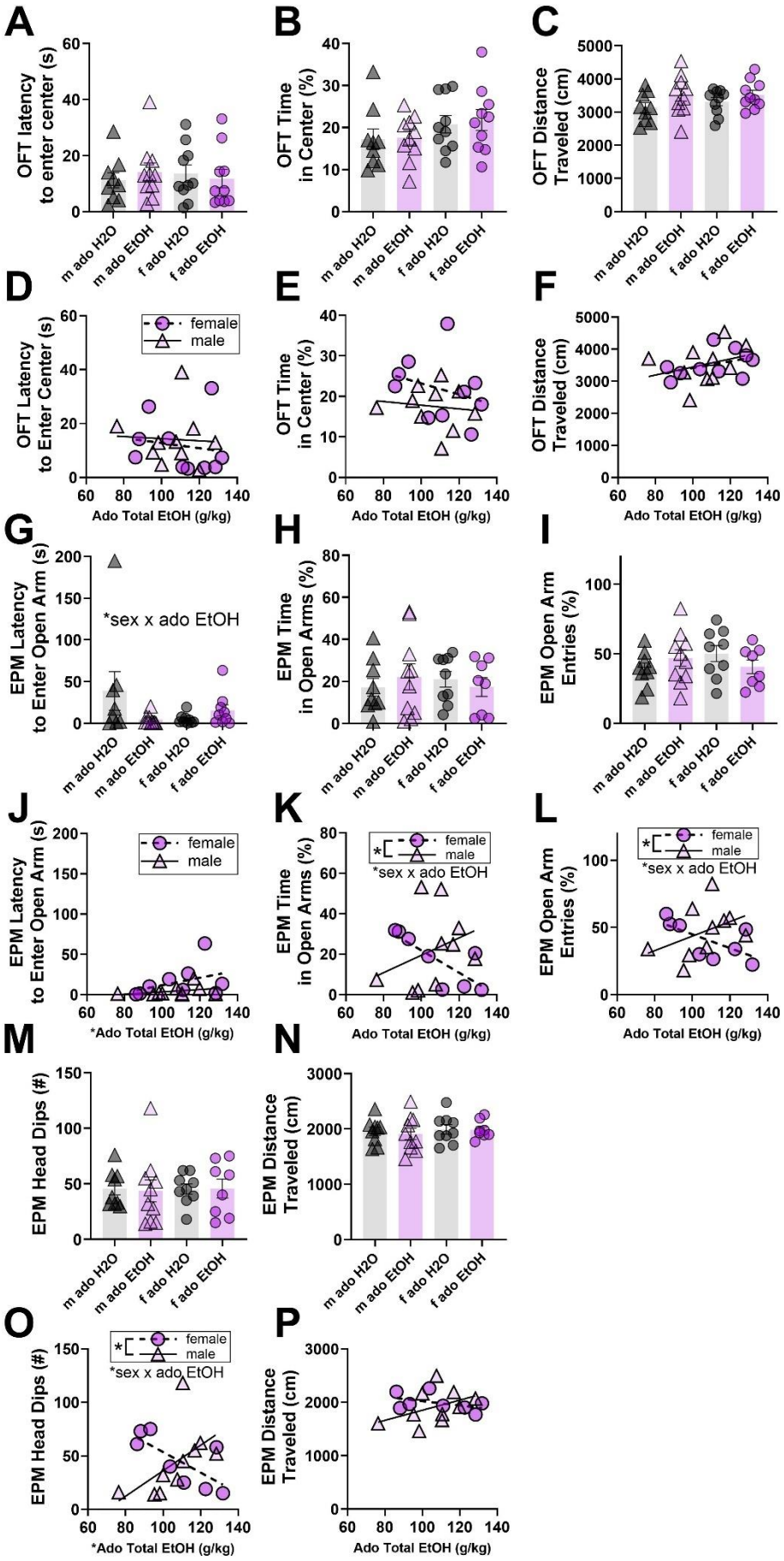
A
OFT latency to enter center (s)
m ado H2O
m ado EtOH
f ado H2O
f ado EtOH
B
OFT Time in Center (%)
C
OFT Distance Traveled (cm)
D
OFT Latency to Enter Center (s)
female
male
Ado Total EtOH (g/kg)
E
OFT Time in Center (%)
F
OFT Distance Traveled (cm)
G
EPM Latency to Enter Open Arm (s)
*sex x ado EtOH
H
EPM Time in Open Arms (%)
I
EPM Open Arm Entries (%)
J
EPM Latency to Enter Open Arm (s)
*Ado Total EtOH (g/kg)
K
EPM Time in Open Arms (%)
L
EPM Open Arm Entries (%)
M
EPM Head Dips (#)
N
EPM Distance Traveled (cm)
O
EPM Head Dips (#)
P
EPM Distance Traveled (cm)

Figure 3: **Adolescent alcohol consumption had sex-specific effects on adult exploratory behaviors. A)** OFT latency to enter center of arena. **(B)** OFT percent time spent in center of arena. **(C)** OFT total distance traveled. **(D)** OFT latency to enter center compared to adolescent EtOH consumption. **(E)** OFT percent time in center compared to adolescent EtOH consumption. **(F)** OFT total distance traveled compared to adolescent EtOH consumption. **G)** EPM latency to enter an open arm. **(H)** EPM percent time spent in open arms. **(I)** EPM percent open arm entries. **(J)** EPM latency to enter an open arm compared to adolescent EtOH consumption. **(K)** EPM percent time spent in open arms compared to adolescent EtOH consumption. **(L)** EPM percent open arm entries compared to adolescent EtOH consumption. **M)** EPM number of head dips. **(N)** EPM total distance traveled. **(O)** EPM number of head dips compared to adolescent EtOH consumption. **(P)** EPM total distance traveled compared to adolescent EtOH consumption. M = male; f = female; ado = adolescent. In scatter plots, a simple linear regression was used to generate lines of best fit and aid interpretation but were independent from statistical analysis. Data are shown as mean +/- SEM. *p<0.05. n=8-10/sex/treatment.

3.4 Adolescent binge drinking led to sex-specific alterations in adult whole-brain functional connectivity and pathway-specific connectivity

A final cohort of mice underwent resting state functional magnetic resonance imaging (rs-fMRI) roughly 30 days after adolescent drinking (**Fig 1C**). The mouse brain was partitioned to 62 bilateral regions of interest (ROIs) anatomically defined in the Allen Mouse Brain Atlas[23] (see **Supplemental Materials** for ROI descriptions). Alcohol consumption, sex, and interactions of alcohol and sex altered whole-brain resting state functional connectivity by a variety of measurements (**Supplemental Materials**). Specifically, females showed a strong brain-wide decrease in overall global functional connectivity post-binge drinking (**Fig 4A-B**), while this pattern was reversed in males (**Fig 4A-B**). Based on the known functional connectivity deficits seen following substance use and our a-priori hypotheses, we further explored this data with the PFC as a seed region (**Fig 5**, **Supplemental Materials**). Here, we saw that female mice showed a decrease and male mice showed an increase in functional connectivity between the PFC and a variety of regions including both dorsal and ventral striatum (**Fig 5, Supplemental Materials**). Supplementary seed analyses confirmed the hippocampus and insula as additional hub regions for adolescent alcohol-associated connectivity changes (**Supplemental Materials**). Together, functional imaging data demonstrates a robust sex-dependent and dose-dependent alteration in whole brain connectivity and PFC connectivity, consistent with sex differences in behavioral profiles.

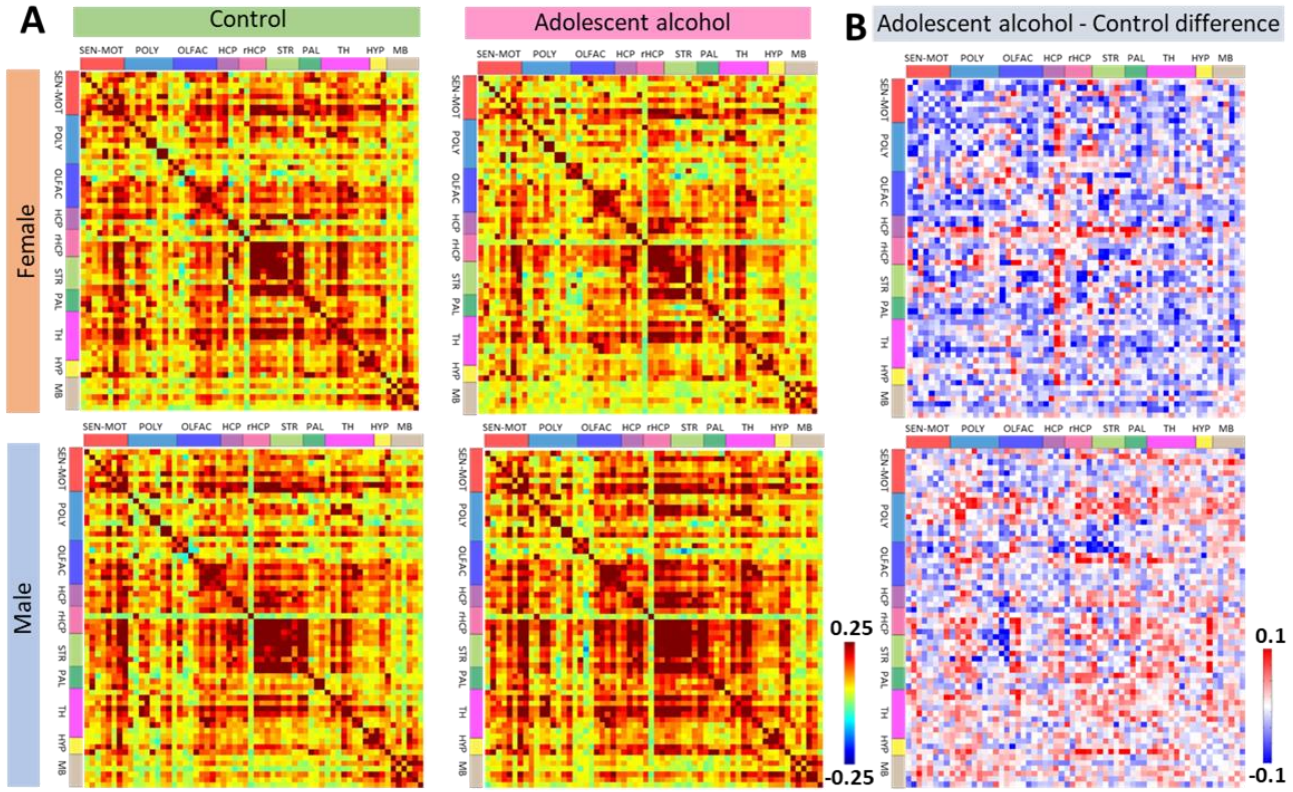

Figure 4. Whole brain functional connectivity differs across sex and due to adolescent alcohol consumption. (A) Average resting state functional connectivity (RSFC) matrices for sex and alcohol groups. The color bar (± 0.25 range) represents the z-score values for the corresponding RSFC. **(B)** Difference of RSFC between alcohol and control groups for each sex. The red-blue color bar (± 0.1 range) shows the z-score differences for the increased or decreased average RSFC in adolescent alcohol-exposed mice in comparison to the controls. n=11 mice/sex/treatment.

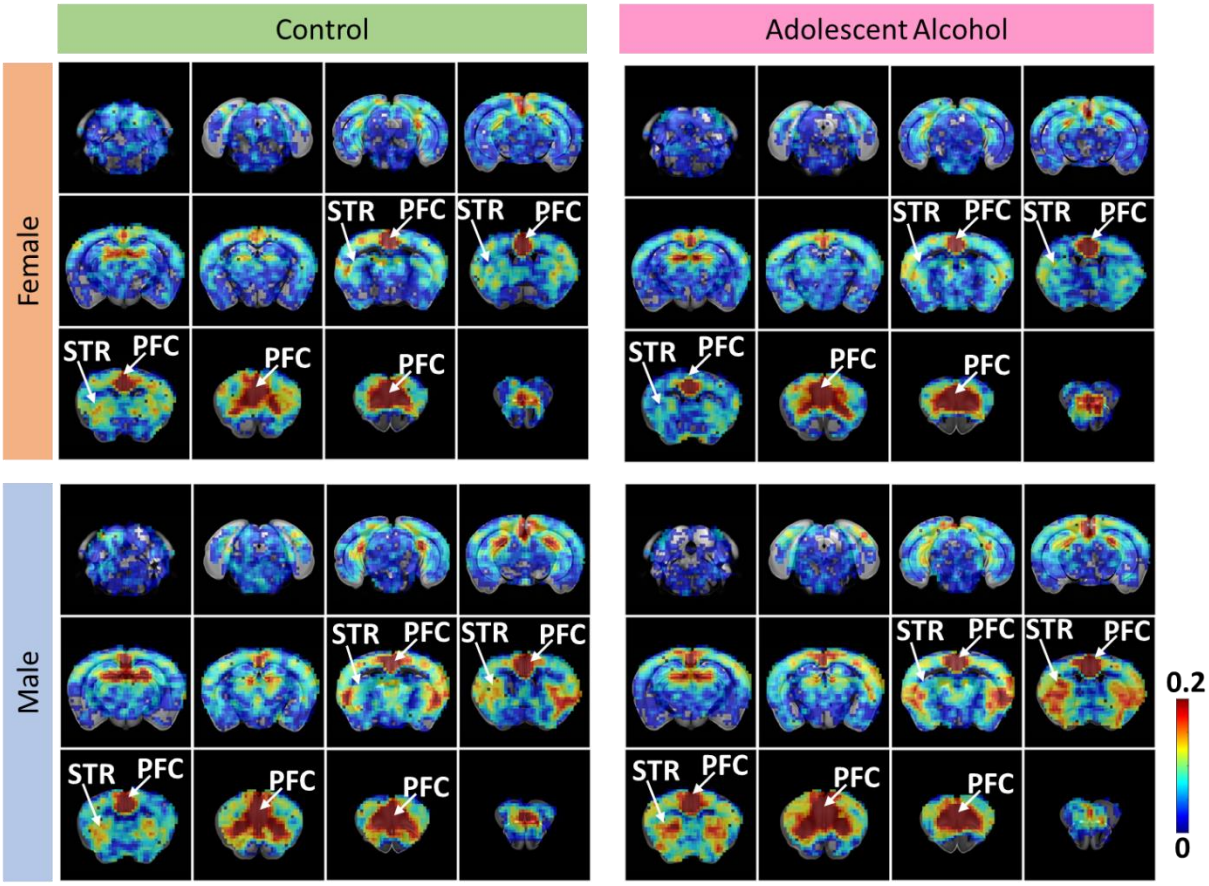

Figure 5. PFC seed-based functional connectivity shows differences in connectivity with key addiction regions, such as the striatum. Average seed-based functional connectivity maps of PFC for sex- and treatment-specific groups**.** Anatomical classification of PFC is available in Supp Fig 9. The color bar (± 0.2 range) represents the average correlation values for the corresponding RSFC between the PFC and all other voxels. PFC and the groups of brain voxels detected as striatum (STR) are indicated with white arrows. n=11 mice/sex/treatment.

4. DISCUSSION

This series of studies tested the relationship between voluntary adolescent alcohol consumption and adult behaviors and whole-brain functional connectivity changes in a mouse model of binge drinking. Adult females with a history of adolescent alcohol consumption had a greater preference for alcohol and quinine-adulterated alcohol than water-exposed controls. Additional OFT and EPM tests revealed complementary sex-specific changes in exploration that were also sensitive to adolescent alcohol dose. fMRI experiments revealed alterations in prefrontal cortical-driven polymodal association network connectivity with brain regions known to be involved in AUD in adult humans, such as the striatum. Cumulatively, these data provide evidence of long-

term disruptions in addiction-related behaviors and brain function attributable to adolescent alcohol exposure, particularly in females.

Our prior work demonstrated that adolescent consumption does not robustly increase adult alcohol consumption across multiple rodent models[16] despite previously identified profound changes in prefrontal cortical function following adolescent alcohol consumption[15]. Replicating our prior data, we found a transient increase in adult alcohol preference, and our current work extends this to demonstrate effects of adolescent alcohol consumption emerge again in the presence of an aversive stimulus during adult drinking. Consumption of alcohol in adulthood without quinine predicted consumption of alcohol with quinine within subjects, supporting that this task may represent behavioral flexibility. Notably, sex differences have been reported in the consumption of alcohol with quinine[24] and sensitivity to the aversive effects of quinine can vary independently of aversion-resistance[25]. Despite some minor limitations of using quinine, our data are consistent with a broader framework that adolescent alcohol exposure impairs adult behavioral flexibility, or the ability to modify behavior in response to changes in an environment[26,27]. This has clear implications for human alcohol use, as a key component of human AUD is the continued use of alcohol despite negative consequences[28]. Our data are further consistent with human data that demonstrate the positive relationship between adolescent binge drinking and later life alcohol use is dramatically stronger in females than in males[3].

We observed that lower adolescent alcohol consumption corresponded to increased adult alcohol consumption. While surprising, this is consistent with our prior data[16]. One possible interpretation is that our outcome variable, adult alcohol consumption, has an inverted U-shaped response curve, whereby adolescent mice may consume such high levels of alcohol in a DID paradigm that dose effects appear to have a negative slope. If this is the case, we would predict that a positive relationship between total adolescent and adult alcohol consumption would exist among rodent models of lower alcohol consumption during adolescence. This may explain some of the inconsistent behavioral effects of different adolescent alcohol exposure paradigms across the literature[29].

Additionally, we report that adolescent alcohol exposure increased exploration in males while decreasing exploration in females, and this scaled with volume of adolescent alcohol consumed. Female-specific decreases in exploration coupled with female-specific susceptibility to aversion-resistant drinking accumulate to indicate

that females with a history of adolescent alcohol use may be vulnerable to substance use through multiple mechanisms. This sheds light on the growing rate of AUD diagnoses in women[30]. However, it is worth noting that prior studies using different adolescent alcohol protocols have reported mixed effects on adult EPM behaviors, with some reporting increased[31], decreased[26], or no changes[32–34] in adult exploratory behaviors. Our data suggest that variability in reported EPM effects may be, in part, attributed to different dosing across alcohol paradigms. It is also possible that behavioral differences were sensitive to the behavioral battery. Further, changes in exploratory behaviors due to adolescent alcohol exposure could be sensitive to specific experimental conditions, a phenomenon that could be particularly pronounced for EPM[35].

Analyses of adolescent alcohol consumption showed reliable binge-like alcohol consumption, as our laboratory has published previously[15,16]. While the DID model allows us to connect voluntary binge alcohol consumption to outcome variables, drawbacks include single housing of animals and potential variability in voluntary consumption across cohorts. In one cohort, we observed significantly elevated alcohol consumption in females, which is consistent with findings from adult rodents[11,36]. However, it is likely that pubertal onset and the beginning of adult hormonal fluctuations contribute to the development of elevated alcohol consumption in females, and the timing of this can vary within individuals[37]. Thus, true sex differences in alcohol consumption may not emerge until post puberty, and varying differences in consumption by biological sex seen across cohorts represent this fluctuating onset and perhaps variable estrous stages.

Whole-brain functional connectivity was assessed to identify changes in neural circuits underlying changes in alcohol preference and exploration. We consistently observed that females showed decreased and males showed increased brain-wide functional connectivity following adolescent binge drinking. We primarily focused our attention and analysis on the PFC and the polymodal association network due to the robust preclinical and human literature on alcohol's effects on the PFC. However, because hippocampal and insular regions emerged as key nodes in our initial unbiased analysis, we conducted additional seed analyses to confirm their complex responses to alcohol use. Broadly, we found an increase in functional connectivity between the PFC and striatum in males, and a decrease of this connectivity in females, following binge alcohol consumption. The anterior cingulate cortex connectivity to the striatum (specifically the lateral septal complex, caudoputamen, nucleus accumbens, and olfactory tubercle) all showed significant main effects from alcohol exposure. Importantly,

human imaging studies on adolescent binge drinkers have also identified the significance of striatal and cortical projections[7,38]. Work by Jones et al.[7] uses a repeated measures design to show impaired developmental maturation of the PFC, including the anterior cingulate cortex, in previously alcohol-naive subjects who participated in regular binge drinking, suggesting that underdevelopment and hypoactivity of the PFC during adolescence is a critical component of the risky decision making seen with drug use. Notably, other adverse early life experiences such as child maltreatment have also been shown to impair prefrontal development[39] and increase risk of substance misuse in women[40,41]. Thus, PFC dysfunction could be a convergent pathway through which child maltreatment and adolescent substance use can uniquely and synergistically increase susceptibility of women to AUD.

The potential association between observed functional connectivity deficits and impaired exploratory behaviors in the elevated plus maze has not been previously studied to our knowledge. Changes in cortico-striatal circuits could feasibly mediate the relationship between adolescent alcohol use and adult exploration in our study[42]. More work has been done to evaluate the links between adolescent alcohol use, behavioral flexibility, and brain functional connectivity[13]. A preclinical study by Gómez and colleagues[27] evaluated the impact of intermittent intragastric adolescent alcohol exposure on adult behavioral flexibility in an attentional set shifting task and brain functional connectivity (under sedation) within the same rats. In this experiment, they found reduced functional connectivity between multiple ROIs, including the prelimbic cortex and the nucleus accumbens, and severity of functional connectivity deficits were associated with reversal learning deficits within subjects in a mediation analysis. Additionally, females had more pronounced reversal deficits than males after adolescent alcohol exposure. Thus, while functional connectivity changes reflect statistical dependencies and not necessarily direct causal relationships, there is a clear link between adolescent alcohol exposure's effects on functional connectivity and behavioral flexibility. These findings are consistent with ours, suggesting that female-specific impairments in behavioral flexibility might also manifest or be related to increased aversion-resistant drinking in adulthood. While aversion-resistant drinking is not a traditional measure of behavioral flexibility, prior literature has demonstrated a biological link between behavioral flexibility and alcohol consumption, where selective breeding of high-alcohol preferring rats also selected for cognitive inflexibility in an attentional set-shifting task[43]. Alternatively, increased aversion-resistant drinking in females could be the

consequences of increased novelty-seeking and a different path to alcohol addiction in females. Importantly, we report consilience in the effects of adolescent alcohol on adult female behavioral flexibility between our study using a voluntary consumption model and others using a forced exposure model. While there are differences between the mouse and human PFC[44], our preclinical rodent model data support the overall human imaging and cognitive processing framework of how adolescent brain function and structure matures over development, and the threat substances of abuse pose for these processes[6,13,45].

To summarize, we found that adolescent binge-like alcohol consumption led to increased aversion-resistant drinking in females, sex-specific changes in exploratory behaviors, and changes in whole brain functional connectivity. These data suggest that females may be more vulnerable to lasting addiction-related behavioral consequences of adolescent alcohol exposure, and these may be driven by functional connectivity changes in prefrontal-striatal circuits. By using a voluntary adolescent alcohol consumption model, we were able to demonstrate nuanced dose effects, supporting that adolescent alcohol exposure can lead to a range of adult phenotypes. Further, this study provides biological targets for future studies evaluating the growing risk of alcohol use and misuse in women.

5. FUNDING

This study was supported by the National Institutes of Health [F32AA031396 (L.S.), P50AA017823 (N.C.), R01AA029403 (N.C), R01AA031472 (N.C. and N.Z.), R01NS07816 (P.J.D.), T32NS115667 (M.S.H.), and T32GM154124 (Y.X.)], the Republic of Türkiye Ministry of National Education Scholarship (H.S.Ü.), the American Heart Association [AHA 24PRE1201066 (M.S.H.)], and the Pennsylvania State University [Student Engagement Network Grant (K.T.), Multi-Campus Research Experience for Undergraduates Fellowship (K.T.), Summer Undergraduate Research Experience Fellowships (B.J.D., E.M.), and The Huck Institutes of the Life Sciences Endowment Funds (N.C)].

6. DECLARATION OF COMPETING INTEREST

The authors declare that they have no competing interests.

7. ACKNOWLEDGEMENTS

We acknowledge the Huck Institutes of the Life Sciences High Field Magnetic Resonance Imaging Core Facility (RRID:SCR_024461) for use of the Bruker Biospec 70/30 and the facility director Thomas Neuberger for help on the imaging protocol and in the facility. We thank Keith Griffith, Sophie Anderlind, and Varya Zlotnik for their technical assistance, and we thank Avery Sicher for her conceptual input.

8. CONTRIBUTIONS

LRS and NAC designed experiments. LRS, HSÜ, YX, KT, BJD, and EPM conducted experiments. LRS, HSÜ, YX, and MSH contributed to analysis. LRS and NAC wrote the manuscript with input from all authors. LRS, YX, MSH, NAC, NZ, and PJD acquired funding.

REFERENCES

(1) DeWit, D. J.; Adlaf, E. M.; Offord, D. R.; Ogborne, A. C. Age at First Alcohol Use: A Risk Factor for the Development of Alcohol Disorders. *AJP* **2000**, *157* (5), 745–750. https://doi.org/10.1176/appi.ajp.157.5.745.

(2) Grant, B. F.; Dawson, D. A. Age at Onset of Alcohol Use and Its Association with DSM-IV Alcohol Abuse and Dependence: Results from the National Longitudinal Alcohol Epidemiologic Survey. *Journal of Substance Abuse* **1997**, *9*, 103–110. https://doi.org/10.1016/S0899-3289(97)90009-2.

(3) Patrick, M. E.; Peterson, S. J.; Pang, Y. C.; Terry-McElrath, Y. M. Links between Adolescent Binge Drinking and Midlife Alcohol Use Behaviors by Age, Sex, and Race/Ethnicity. *Alcohol, Clinical and Experimental Research* **2024**, *48* (11), 2060–2069. https://doi.org/10.1111/acer.15435.

(4) Spear, L. P. Adolescent Neurodevelopment. *Journal of Adolescent Health* **2013**, *52* (2, Supplement 2), S7–S13. https://doi.org/10.1016/j.jadohealth.2012.05.006.

(5) Sun, D.; Adduru, V. R.; Phillips, R. D.; Bouchard, H. C.; Sotiras, A.; Michael, A. M.; Baker, F. C.; Tapert, S. F.; Brown, S. A.; Clark, D. B.; Goldston, D.; Nooner, K. B.; Nagel, B. J.; Thompson, W. K.; De Bellis, M. D.; Morey, R. A. Adolescent Alcohol Use Is Linked to Disruptions in Age-Appropriate Cortical Thinning: An Unsupervised Machine Learning Approach. *Neuropsychopharmacology* **2023**, *48* (2), 317–326. https://doi.org/10.1038/s41386-022-01457-4.

(6) Müller-Oehring, E. M.; Kwon, D.; Nagel, B. J.; Sullivan, E. V.; Chu, W.; Rohlfing, T.; Prouty, D.; Nichols, B. N.; Poline, J.-B.; Tapert, S. F.; Brown, S. A.; Cummins, K.; Brumback, T.; Colrain, I. M.; Baker, F. C.; De Bellis, M. D.; Voyvodic, J. T.; Clark, D. B.; Pfefferbaum, A.; Pohl, K. M. Influences of Age, Sex, and Moderate Alcohol Drinking on the Intrinsic Functional Architecture of Adolescent Brains. *Cereb Cortex* **2018**, *28* (3), 1049–1063. https://doi.org/10.1093/cercor/bhx014.

(7) Jones, S. A.; Cservenka, A.; Nagel, B. J. Binge Drinking Impacts Dorsal Striatal Response during Decision Making in Adolescents. *Neuroimage* **2016**, *129*, 378–388. https://doi.org/10.1016/j.neuroimage.2016.01.044.

(8) Kushner, M. G.; Maurer, E.; Menary, K.; Thuras, P. Vulnerability to the Rapid ("Telescoped") Development of Alcohol Dependence in Individuals with Anxiety Disorder. *J. Stud. Alcohol Drugs* **2011**, *72* (6), 1019–1027. https://doi.org/10.15288/jsad.2011.72.1019.

(9) Kushner, M. G.; Abrams, K.; Borchardt, C. The Relationship between Anxiety Disorders and Alcohol Use Disorders: A Review of Major Perspectives and Findings. *Clinical Psychology Review* **2000**, *20* (2), 149–171. https://doi.org/10.1016/S0272-7358(99)00027-6.

(10) Koob, G. F. The Dark Side of Emotion: The Addiction Perspective. *European Journal of Pharmacology* **2015**, *753*, 73–87. https://doi.org/10.1016/j.ejphar.2014.11.044.

(11) Rhodes, J. S.; Best, K.; Belknap, J. K.; Finn, D. A.; Crabbe, J. C. Evaluation of a Simple Model of Ethanol Drinking to Intoxication in C57BL/6J Mice. *Physiology & Behavior* **2005**, *84* (1), 53–63. https://doi.org/10.1016/j.physbeh.2004.10.007.

(12) Liu, Y.; Perez, P. D.; Ma, Z.; Ma, Z.; Dopfel, D.; Cramer, S.; Tu, W.; Zhang, N. An Open Database of Resting-State fMRI in Awake Rats. *NeuroImage* **2020**, *220*, 117094. https://doi.org/10.1016/j.neuroimage.2020.117094.

(13) Geier, C. F. Adolescent Cognitive Control and Reward Processing: Implications for Risk Taking and Substance Use. *Horm Behav* **2013**, *64* (2), 333–342. https://doi.org/10.1016/j.yhbeh.2013.02.008.

(14) Crowley, N. A.; Dao, N. C.; Magee, S. N.; Bourcier, A. J.; Lowery-Gionta, E. G. Animal Models of Alcohol Use Disorder and the Brain: From Casual Drinking to Dependence. *Translational Issues in Psychological Science* **2019**, *5* (3), 222–242. https://doi.org/10.1037/tps0000198.

(15) Sicher, A. R.; Starnes, W. D.; Griffith, K. R.; Dao, N. C.; Smith, G. C.; Brockway, D. F.; Crowley, N. A. Adolescent Binge Drinking Leads to Long-Lasting Changes in Cortical Microcircuits in Mice. *Neuropharmacology* **2023**, *234*, 109561. https://doi.org/10.1016/j.neuropharm.2023.109561.

(16) Sicher, A. R.; Liss, A.; Vozella, V.; Marsland, P.; Seemiller, L. R.; Springer, M.; Starnes, W. D.; Griffith, K. R.; Smith, G. C.; Astefanous, A.; Deak, T.; Roberto, M.; Varodayan, F. P.; Crowley, N. A. Voluntary Adolescent Alcohol Exposure Does Not Robustly Increase Adulthood Consumption of Alcohol in Multiple Mouse and Rat Models. *Addiction Neuroscience* **2024**, *12*, 100171. https://doi.org/10.1016/j.addicn.2024.100171.

(17) Dao, N. C.; Suresh Nair, M.; Magee, S. N.; Moyer, J. B.; Sendao, V.; Brockway, D. F.; Crowley, N. A. Forced Abstinence From Alcohol Induces Sex-Specific Depression-Like Behavioral and Neural Adaptations in Somatostatin Neurons in Cortical and Amygdalar Regions. *Frontiers in Behavioral Neuroscience* **2020**, *14*.

(18) Brockway, D. F.; Griffith, K. R.; Aloimonos, C. M.; Clarity, T. T.; Moyer, J. B.; Smith, G. C.; Dao, N. C.; Hossain, M. S.; Drew, P. J.; Gordon, J. A.; Kupferschmidt, D. A.; Crowley, N. A. Somatostatin Peptide Signaling Dampens Cortical Circuits and Promotes Exploratory Behavior. *Cell Rep* **2023**, *42* (8), 112976. https://doi.org/10.1016/j.celrep.2023.112976.

(19) Carola, V.; D'Olimpio, F.; Brunamonti, E.; Mangia, F.; Renzi, P. Evaluation of the Elevated Plus-Maze and Open-Field Tests for the Assessment of Anxiety-Related Behaviour in Inbred Mice. *Behavioural Brain Research* **2002**, *134* (1), 49–57. https://doi.org/10.1016/S0166-4328(01)00452-1.

(20) Tsao, C.-H.; Flint, J.; Huang, G.-J. Influence of Diurnal Phase on Behavioral Tests of Sensorimotor Performance, Anxiety, Learning and Memory in Mice. *Sci Rep* **2022**, *12* (1), 432. https://doi.org/10.1038/s41598-021-03155-5.

(21) Mathis, A.; Mamidanna, P.; Cury, K. M.; Abe, T.; Murthy, V. N.; Mathis, M. W.; Bethge, M. DeepLabCut: Markerless Pose Estimation of User-Defined Body Parts with Deep Learning. *Nat Neurosci* **2018**, *21* (9), 1281–1289. https://doi.org/10.1038/s41593-018-0209-y.

(22) Power, J. D.; Barnes, K. A.; Snyder, A. Z.; Schlaggar, B. L.; Petersen, S. E. Spurious but Systematic Correlations in Functional Connectivity MRI Networks Arise from Subject Motion. *Neuroimage* **2012**, *59* (3), 2142–2154. https://doi.org/10.1016/j.neuroimage.2011.10.018.

(23) Lein, E. S.; Hawrylycz, M. J.; Ao, N.; Ayres, M.; Bensinger, A.; Bernard, A.; Boe, A. F.; Boguski, M. S.; Brockway, K. S.; Byrnes, E. J.; Chen, L.; Chen, L.; Chen, T.-M.; Chi Chin, M.; Chong, J.; Crook, B. E.; Czaplinska, A.; Dang, C. N.; Datta, S.; Dee, N. R.; Desaki, A. L.; Desta, T.; Diep, E.; Dolbeare, T. A.; Donelan, M. J.; Dong, H.-W.; Dougherty, J. G.; Duncan, B. J.; Ebbert, A. J.; Eichele, G.; Estin, L. K.; Faber, C.; Facer, B. A.; Fields, R.; Fischer, S. R.; Fliss, T. P.; Frensley, C.; Gates, S. N.; Glattfelder, K. J.; Halverson, K. R.; Hart, M. R.; Hohmann, J. G.; Howell, M. P.; Jeung, D. P.; Johnson, R. A.; Karr, P. T.; Kawal, R.; Kidney, J. M.; Knapik, R. H.; Kuan, C. L.; Lake, J. H.; Laramee, A. R.; Larsen, K. D.; Lau, C.; Lemon, T. A.; Liang, A. J.; Liu, Y.; Luong, L. T.; Michaels, J.; Morgan, J. J.; Morgan, R. J.; Mortrud, M. T.; Mosqueda, N. F.; Ng, L. L.; Ng, R.; Orta, G. J.; Overly, C. C.; Pak, T. H.; Parry, S. E.; Pathak, S. D.; Pearson, O. C.; Puchalski, R. B.; Riley, Z. L.; Rockett, H. R.; Rowland, S. A.; Royall, J. J.; Ruiz, M. J.; Sarno, N. R.; Schaffnit, K.; Shapovalova, N. V.; Sivisay, T.; Slaughterbeck, C. R.; Smith, S. C.; Smith, K. A.; Smith, B. I.; Sodt, A. J.; Stewart, N. N.; Stumpf, K.-R.; Sunkin, S. M.; Sutram, M.; Tam, A.; Teemer, C. D.; Thaller, C.; Thompson, C. L.; Varnam, L. R.; Visel, A.; Whitlock, R. M.; Wohnoutka, P. E.; Wolkey, C. K.; Wong, V. Y.; Wood, M.; Yaylaoglu, M. B.; Young, R. C.; Youngstrom, B. L.; Feng Yuan, X.; Zhang, B.; Zwingman, T. A.; Jones, A. R. Genome-Wide Atlas of Gene Expression in the Adult Mouse Brain. *Nature* **2007**, *445* (7124), 168–176. https://doi.org/10.1038/nature05453.

(24) Fulenwider, H. D.; Nennig, S. E.; Price, M. E.; Hafeez, H.; Schank, J. R. Sex Differences in Aversion-Resistant Ethanol Intake in Mice. *Alcohol and Alcoholism* **2019**, *54* (4), 345–352. https://doi.org/10.1093/alcalc/agz022.

(25) Cicala, G. A.; McMichael, J. S. Quinine Aversion Thresholds in Rats as a Function of Age and Psychophysical Procedure. *Canadian Journal of Psychology / Revue canadienne de psychologie* **1964**, *18* (1), 28–35. https://doi.org/10.1037/h0083293.

(26) Varlinskaya, E. I.; Hosová, D.; Towner, T.; Werner, D. F.; Spear, L. P. Effects of Chronic Intermittent Ethanol Exposure during Early and Late Adolescence on Anxiety-like Behaviors and Behavioral Flexibility in Adulthood. *Behav Brain Res* **2020**, *378*, 112292. https://doi.org/10.1016/j.bbr.2019.112292.

(27) Gómez-A, A.; Dannenhoffer, C. A.; Elton, A.; Lee, S.-H.; Ban, W.; Shih, Y.-Y. I.; Boettiger, C. A.; Robinson, D. L. Altered Cortico-Subcortical Network After Adolescent Alcohol Exposure Mediates Behavioral Deficits in Flexible Decision-Making. *Front. Pharmacol.* **2021**, *12*. https://doi.org/10.3389/fphar.2021.778884.

(28) Association, A. P. *Diagnostic and Statistical Manual of Mental Disorders : DSM-5*; American Psychiatric Association, 2013.

(29) Spear, L. P. Effects of Adolescent Alcohol Consumption on the Brain and Behaviour. *Nat Rev Neurosci* **2018**, *19* (4), 197–214. https://doi.org/10.1038/nrn.2018.10.

(30) Grant, B. F.; Chou, S. P.; Saha, T. D.; Pickering, R. P.; Kerridge, B. T.; Ruan, W. J.; Huang, B.; Jung, J.; Zhang, H.; Fan, A.; Hasin, D. S. Prevalence of 12-Month Alcohol Use, High-Risk Drinking, and DSM-IV Alcohol Use Disorder in the United States, 2001-2002 to 2012-2013: Results From the National

Epidemiologic Survey on Alcohol and Related Conditions. *JAMA Psychiatry* **2017**, *74* (9), 911–923. https://doi.org/10.1001/jamapsychiatry.2017.2161.

(31) Healey, K. L.; Kibble, S. A.; Bell, A.; Kramer, G.; Maldonado-Devincci, A.; Swartzwelder, H. S. Sex Differences in the Effects of Adolescent Intermittent Ethanol Exposure on Exploratory and Anxiety-like Behavior in Adult Rats. *Alcohol* **2022**, *98*, 43–50. https://doi.org/10.1016/j.alcohol.2021.11.002.

(32) Seemiller, L. R.; Garcia-Trevizo, P.; Novoa, C.; Goldberg, L. R.; Murray, S.; Gould, T. J. Adolescent Intermittent Alcohol Exposure Produces Strain-Specific Cross-Sensitization to Nicotine and Other Behavioral Adaptations in Adulthood in C57BL/6J and DBA/2J Mice. *Pharmacology Biochemistry and Behavior* **2023**, *232*, 173655. https://doi.org/10.1016/j.pbb.2023.173655.

(33) Torcaso, A.; Asimes, A.; Meagher, M.; Pak, T. R. Adolescent Binge Alcohol Exposure Increases Risk Assessment Behaviors in Male Wistar Rats after Exposure to an Acute Psychological Stressor in Adulthood. *Psychoneuroendocrinology* **2017**, *76*, 154–161. https://doi.org/10.1016/j.psyneuen.2016.11.032.

(34) Younis, R. M.; Wolstenholme, J. T.; Bagdas, D.; Bettinger, J. C.; Miles, M. F.; Damaj, M. I. Adolescent but Not Adult Ethanol Binge Drinking Modulates Ethanol Behavioral Effects in Mice Later in Life. *Pharmacology Biochemistry and Behavior* **2019**, *184*, 172740. https://doi.org/10.1016/j.pbb.2019.172740.

(35) Initiative, T. B. R.; Amaral, O. B.; Carneiro, C. F. D.; Neves, K.; Sampaio, A. P. W.; Gomes, B. V.; Abreu, M. B. de; Tan, P. B.; Mota, G. P. S.; Goulart, R. N.; Fernandes, N. R. de S.; Linhares, J. H.; Ibelli, A. M. G.; Sebollela, A.; Andricopulo, A. D.; Carvalho, A. A. V. de; Silva, A. P. e; Souza, A. S. O.; Lima, A. C. C. de; Sousa, A. M. de; Birbrair, A.; Borbely, A. U.; Machado, A. M.; Costa, A. do C.; Vasconcelos, A. P. de; Silva, A. H. B. de L.; Souza, A. de; Herrmann, A. P.; Bastos, A. P. A.; Nunes, A. C. C.; Castrucci, A. M. de L.; Paula, A. B. R.; Waltrick, A. P. F.; Macedo, A. G. F. de; Mecawi, A. S.; Rinaldi, A. W.; Canedo, A. D.; Vidigal, A. P. P.; Marcal, A. P.; Monteiro, A. M.; Rocha, B. G. S.; Pachane, B. C.; Andrade, B. da S.; Casali, B. C.; Popik, B.; Souza, C. P. de; Santos, C. da S. dos; Goncalves, C. M.; Nascimento, C. R. B. do; Verissimo, C. P.; Girardi, C. E. N.; Penido, C.; Batista, C.; Saibro-Girardi, C.; Pedrosa, C. da S. G.; Panis, C.; Picoli, C. de C.; Furini, C. R. G.; Caetano, D. S. L.; Gelain, D. P.; Silva, D. C.; Aguiar, D. C. de; Goncalves, D. A.; Silva, D. S. da; Araujo, D. A. M. D.; Junior, D. A. C.; Campos, D. B. P. de; Nachtigall, E. G.; Tanabe, E. L. L.; Kioshima, E. S.; Seiva, F. R. F.; Mendes, F. de A.; Silva, F. J. M. da; Moreira, F. de A.; Vanz, F.; Leser, F. S.; Ferrao, F. M.; Lotz, F. N.; Silva, F. C. dos S.; Bloise, F. F.; Lima, F. R. S.; Lara, F. A.; Volpato, F. A.; Stefanello, F. M.; Vitorino, F. N. de L.; Fonseca, F. N.; Furtado, G. V.; Neves, G. A.; Zanetti, G.; Cancelliero, G. S.; Pisani, G. F. D.; Casagrande, G. C. A.; Villas-Boas, G. R.; Cruz, H. R. O. A. da; Borges, H. L.; Araujo, H. S. S. D.; Povoa, H. C. C.; Brunel, H. dos S. S.; Bayer, H.; Baptista, I. L.; Werle, I.; Divino, I. A.; Jardim, I. A. B. A.; Zanoveli, J. M.; Peixoto, J. de O.; Rinaldi, J. de C.; Ferreira, J. B.; Franco, J. L.; Rugani, J. M. N.; Cruz, J. V. R.; Myskiw, J. de C.; Quillfeldt, J. A.; Costa, J. M. J. P. da; Barros, J. H. O. de; Barros, J. M.; Cunha, J. P. C. da; Ayub, J. G. M.; Freitas, J. D. R. de; Roson, J. N.; Borbely, K. S. C.; Asensi, K. D.; Queiroz, K. B. de; Rodrigues, K. dos S.; Vieira, K. de C.; Guerra, K. T. K.; Pires, K. S. N.; Trajano-Silva, L. A. M.; Bertoglio, L. J.; Assis, L. V. M. de; Lery, L. M. S.; Vasconcelos, L. M.; Silva, L. de O. M. da; Fernandes-Siqueira, L. de O.; Alvares, L. D. O.; Falcione, L. H. de M.; Silva, L. dos S. da; Vieira, L. G.; Madeira, L. F.; Nunes, L. E. D.; Chuffa, L. G. de A.; Behrens, L. M. P.; Esteca, M. V.; Felipe, M. S. S.; Moraes, M. N.; Saraiva-Pereira, M. L.; Silveira, M. S. da; Duarte, M. S. V.; Porcionatto, M. A.; Salvi, M.; Clavero, M. A.; Ferreira, M. L.; Gallas-Lopes, M.; Moura, M. A. de; Isoldi, M. C.; Mundim, M. T. V. V.; Andrades, M.; Donato, M. F.; Barboza, M. P.; Fagundes, M. M. de A.; Silva, M. A.; Ledur, M. C.; Silva, M. D. da; Baqui, M. M. A.; Souza, M. P. de; Povoa, N. I. L. P.; Bellini, N. K.; Pedra, N. S.; Somensi, N.; Soares, N. P.; Nunes, N. M. P.; Silva, N. F.; Carvalho, P. M. G. de; Cappelletti, P. A.; Garcez, P. P.; Martins, P. R.; Brito, P. K. M. O.; Lauar, P. R. M.; Nicolicht-Amorim, P.; Chitolina, R.; Barbosa, R. A. Q.; Cordova, R. A. G.; Goldenberg, R. C. D. S.; Tavares, R. G.; Saito, R. de F.; Krogh, R.; Andreatini, R.; Almeida, R. F.; Menezes, R. C. A. de; Rorato, R.; Chammas, R.; Andrade, R. V. de; Spanevello, R. M.; Costa, R. A.; Monte-Neto, R. L. do; Reis, S. A. dos; Kraus, S. I.; Silva, S. C.; Michelan-Duarte, S.; Rehen, S. K.; Noronha, S. I. S. R. de; Ortiga-Carvalho, T. M.; Prieto, T. da S.; Fagundes, T. R.; Nakamura, T. K. E.; Costa, T. E. M. M.; Junior, T. C. T.; Luz, T. B. da; Silva, T. A. da; Santos, T. G. D.; Beijamini, V.; Monteiro, V. R. de S.; Wippel, V. A.; Valenca, V. M. O.; Altei, W. F. Estimating the Replicability of Brazilian Biomedical Science. bioRxiv April 8, 2025, p 2025.04.02.645026. https://doi.org/10.1101/2025.04.02.645026.

(36) Satta, R.; Hilderbrand, E. R.; Lasek, A. W. Ovarian Hormones Contribute to High Levels of Binge-Like Drinking by Female Mice. *Alcoholism: Clinical and Experimental Research* **2018**, *42* (2), 286–294. https://doi.org/10.1111/acer.13571.
(37) Witt, E. D. Puberty, Hormones, and Sex Differences in Alcohol Abuse and Dependence. *Neurotoxicology and Teratology* **2007**, *29* (1), 81–95. https://doi.org/10.1016/j.ntt.2006.10.013.
(38) Morales, A. M.; Stark, N. A.; Nagel, B. J. Ventral Striatal Resting-State Functional Connectivity in Adolescents Is Associated with Earlier Onset of Binge Drinking. *Drug Alcohol Depend* **2021**, *227*, 109010. https://doi.org/10.1016/j.drugalcdep.2021.109010.
(39) Teicher, M. H.; Samson, J. A.; Anderson, C. M.; Ohashi, K. The Effects of Childhood Maltreatment on Brain Structure, Function and Connectivity. *Nat Rev Neurosci* **2016**, *17* (10), 652–666. https://doi.org/10.1038/nrn.2016.111.
(40) Kisely, S.; Strathearn, L.; Najman, J. The Influence of Child Maltreatment on Substance or Alcohol Use in 30-Year-Old Adults: A Birth Cohort Study. *Drug Alcohol Rev* **2021**, *40* (4), 673–680. https://doi.org/10.1111/dar.13192.
(41) Guinle, M. I. B.; Sinha, R. The Role of Stress, Trauma, and Negative Affect in Alcohol Misuse and Alcohol Use Disorder in Women. *Alcohol Res* **2020**, *40* (2), 05. https://doi.org/10.35946/arcr.v40.2.05.
(42) Braz, B. Y.; Galiñanes, G. L.; Taravini, I. R.; Belforte, J. E.; Murer, M. G. Altered Corticostriatal Connectivity and Exploration/Exploitation Imbalance Emerge as Intermediate Phenotypes for a Neonatal Dopamine Dysfunction. *Neuropsychopharmacol* **2015**, *40* (11), 2576–2587. https://doi.org/10.1038/npp.2015.104.
(43) De Falco, E.; White, S. M.; Morningstar, M. D.; Ma, B.; Nkurunziza, L. T.; Ahmed-Dilibe, A.; Wellman, C. L.; Lapish, C. C. Impaired Cognitive Flexibility and Heightened Urgency Are Associated with Increased Alcohol Consumption in Rodent Models of Excessive Drinking. *Addiction Biology* **2021**, *26* (5), e13004. https://doi.org/10.1111/adb.13004.
(44) Laubach, M.; Amarante, L. M.; Swanson, K.; White, S. R. What, If Anything, Is Rodent Prefrontal Cortex? *eNeuro* **2018**, *5* (5). https://doi.org/10.1523/ENEURO.0315-18.2018.
(45) Zhao, Q.; Sullivan, E. V.; Műller-Oehring, E.; Honnorat, N.; Adeli, E.; Podhajsky, S.; Baker, F. C.; Colrain, I. M.; Prouty, D.; Tapert, S. F.; Brown, S. A.; Meloy, M. J.; Brumback, T.; Nagel, B. J.; Morales, A. M.; Clark, D. B.; Luna, B.; De Bellis, M. D.; Voyvodic, J. T.; Pfefferbaum, A.; Pohl, K. M. Adolescent Alcohol Use Disrupts Functional Neurodevelopment in Sensation Seeking Girls. *Addict Biol* **2021**, *26* (2), e12914. https://doi.org/10.1111/adb.12914.

Adolescent alcohol consumption alters sex-specific behaviors associated with prefrontal functional connectivity in mice

Running title: adolescent alcohol behavior and imaging

Seemiller et al.

Supplementary Materials

Supplementary Methods:

Extended fMRI methods

fMRI acclimation and data acquisition: Mice were acclimated to the imaging environment for 4 days prior to testing. Briefly, mice were anesthetized with 3% isoflurane while their limbs were lightly bound using surgical tape. Mice were gently positioned in a cylindrical restrainer tube and secured with a bite bar. After mice awoke from anesthesia (assessed by recovery of awake respiration rate, usually 10-20 mins), they were monitored while acclimating for increasing amounts of time. Specifically, mice were restrained for 15, 30, 45, and 60 min on acclimation days 1-4, respectively, while a soundtrack of fMRI noises was played. Afterward, on PND 83-88 (at least 30 days after DID), awake resting state imaging was then performed using a 7T MRI system and Bruker Console (Billerica, MA) using Paravision 7.0.0. Again, mice were briefly anesthetized with 3% isoflurane while being restrained. Once restrained, anesthesia was stopped and mice were allowed to wake up before imaging. A gradient-echo echo-planar imaging (GE-EPI) sequence for T2*-weighted resting-state scans was used for data collection (repetition time (TR) = 1.5 s; echo time (TE) = 15 ms; field of view (FOV) = 1.6 × 1.6 cm; image matrix size 64 x 64; slice number = 16; slice thickness 0.75 mm; slice gap = 0 mm). Each scan lasted 10 min and collected 400 volumes, with three scans per mouse. Rapid imaging with refocused echoes (RARE) was used to acquire T1-weighted anatomical images (TR = 1.5 s; TE = 8 ms; FOV = 1.6 × 1.6 cm; image matrix size = 128 × 128; slice number = 16; slice thickness = 0.75 mm; RARE factor = 8; repetition number = 6; slice gap = 0 mm).

fMRI image preprocessing: Framewise displacement (FD) was calculated to quantify motion (Power et al. 2012): $FD = |\Delta x| + |\Delta y| + |\Delta z| + r * (|\Delta\alpha| + |\Delta\beta| + |\Delta\gamma|)$. r = 2 mm represents the length from the cortex to the center of the brain. Δx, Δy, and Δz (translation distances) and Δα, Δβ, and Δγ (rotations) across x, y, and z axis were calculated using "imregtform" geometric transformation function in MATLAB version R2023b (The MathWorks Inc., Natick, MA, United States). Volumes exhibiting motion over half of the in-plane voxel size (0.125mm) and their temporally adjacent volumes were removed from analysis. Data were manually co-registered to a reference template for anatomical assessment and normalized to Allen Mouse Brain Atlas (Lein et al. 2007) using a custom-developed MATLAB program (Liu et al. 2020). Motion calculation and correction were performed using the Statistical Parametric Mapping (SPM12) package (http://www.fil.ion.ucl.ac.uk/spm/). We performed spatial smoothing using a Gaussian kernel (full-width-half-maximum = 0.375mm, 1.5x the x-y plane voxel size). We performed nuisance regression to eliminate signals originating from white matter (WM) and ventricle voxels, thereby reducing physiological noise (respiration, heart rate, etc.), along with regressing out the six motion parameters for each fMRI frame. Finally, a band-pass filter (0.01-0.1 Hz) was used. For consistency across data sets, 350 volumes from each scan (originally containing 400 volumes) were used.

fMRI image postprocessing: A total of 62 regions of interest (ROIs) were defined based on definitions from the Allen Mouse Brain Atlas (Lein et al. 2007). ROIs were assigned to 10 brain systems: hippocampal region, retrohippocampal region, striatum, sensory-motor cortex, polymodal association cortex, olfactory cortex, pallidum, thalamus, hypothalamus, and midbrain. Resting state functional connectivity between brain regions was analyzed using an ROI-based approach specifically testing Pearson correlations between the average activity time course between each ROI pair. Functional connectivity matrices were calculated using Fisher's z-transformed Pearson's correlation coefficients within each mouse. Seed-based functional connectivity analysis was also used to directly determine regions with strong functional connectivity with the prefrontal cortex. Three scans were collected per mouse, with each scan lasting 10 minutes. After applying motion scrubbing and excluding scans with more than 10% of volumes discarded, all animals retained at least one scan that could be included in the analysis. The total

number of usable scans per group was as follows: alcohol female (11 mice): 30 scans, alcohol male (11 mice): 31 scans, control female (11 mice): 27 scans, and control male (11 mice): 30 scans.

Drinking data analysis

Drinking values that exceeded 2 g within 2 hr (roughly 100 g/kg for a 20 g mouse) were categorized as leaks and removed from drinking analyses. This drinking outlier threshold is consistent with our prior work (Sicher et al. 2024) that found consistent convergence in outliers identified through this method and the ROUT outlier method. These occasional missing data points (< 2% of DID data) due to bottle leakage were omitted in most drinking analyses and imputed as the average of related drinking values in analyses of total amounts consumed. Outliers for adult outcomes were identified in the ROUT outlier test (Q=1%), and mice had to be outliers across more than one measurement within the same test to be excluded. No mice met these criteria in main text Figs 2-3.

OFT and EPM behavior data analysis

Experiments were video-recorded by a camera with a frame rate of 33.6 frames per second. Behaviors were tracked using DeepLabCut (V2.2.1). The head, middle of body, and trunk of the tail were tracked throughout experiments. Tracking employed transfer learning to retrain residual network EfficientNet-B0 (effnet_b0). Training was sufficient when confidence in the position was >99%. Data were exported as a CSV file and analyzed in MATLAB.

Across both OFT and EPM tests, the Euclidean distance of the middle of the body between frames was classified as the distance traveled. The number of frames that a mouse was in the polygon bounded by the zone of interest was used to calculate time spent in a zone of interest. Pixels/frame was converted to cm/s using known arena measurements and camera frame rate. Randomly selected videos were hand-scored and used to validate automated behavior analysis.

OFT and EPM 24 hr after adolescent DID

As described in the main text, male and female C57BL/6J mice were bred in-house, weaned and moved into single housing on a reverse light cycle on PND 21, and underwent DID PND 29-53 (+/- 1 day). One day after the last alcohol access session and the conclusion of DID (PND 53 +/- 1), mice underwent OFT and EPM testing. One subject jumped out of the OFT box during testing, so OFT time in center and distance traveled were not collected for that mouse. Statistical analysis and outlier testing was done as described in the main text. No outliers were detected for OFT or EPM data sets.

OFT and EPM 30 days after adult DID

For adult experiments, male and female C57BL/6J mice were ordered from Jackson Laboratory (Bar Harbor, ME, USA). At least one week prior to DID, subjects were moved and single housed in a reversed light cycle room. DID was conducted as described in the main text, except that it occurred during adulthood (PND 62-86). OFT and EPM testing began on PND 118. Statistical analysis and outlier testing was performed as described in the main text. No mice fell of the EPM, however one outlier subject was removed from EPM analysis.

Supplementary Results:

3.1 Adolescent binge drinking led to minor differences in sex-specific physiological growth

During adolescent DID, alcohol consumption across all cohorts was affected by day (Cohort 1: $F_{6,106} = 8.1$, $p < 0.0001$; Cohort 2: $F_{7,129} = 11.3$, $p < 0.0001$; Cohort 3: $F_{15,150} = 10.8$, $p < 0.0001$). Females weighed less than males (Cohort 1: $F_{1,33} = 37.4$, $p < 0.0001$; Cohort 2: $F_{1,36} = 42.2$, $p < 0.0001$; Cohort 3: $F_{1,40} = 71.6$, $p < 0.0001$) and body weights changed across weeks (Cohort 1: $F_{2,58} = 214.5$, $p < 0.0001$; Cohort 2: $F_{2,76} = 289.8$, $p < 0.0001$; Cohort 3: $F_{2,77} = 462.8$, $p < 0.0001$). Body weights were also significantly impacted by week in the

sex-specific analysis of cohort 1 (female: $F_{2,43} = 300.1$, $p < 0.0001$; male: $F_{2,24} = 62.8$, $p < 0.0001$). Further, body weights were influenced by an interaction of week and sex (Cohort 1: $F_{3,99} = 3.1$, $p = 0.0308$; Cohort 2: $F_{3,108} = 3.8$, $p = 0.0129$; Cohort 3: $F_{3,120} = 8.9$, $p < 0.0001$). *Data are represented in* ***Fig 1*** *of the main text*.

Dependent variable	Effect	F (DFn, DFd)	p
Ado DID EtOH – experiment 1 (Fig 1B) 2-way (Day, Sex) ANOVA	Day	F (5.648, 105.8) = 8.129	<0.0001
	Sex	F (1, 19) = 10.21	0.0048
	Day x Sex	F (15, 281) = 0.6743	0.8092
Body weight – experiment 1 (Fig 1C) 3-way (Week, Sex, Treatment) ANOVA	Week	F (1.757, 57.99) = 214.5	<0.0001
	Sex	F (1, 33) = 37.41	<0.0001
	Treatment	F (1, 33) = 0.02298	0.8804
	Week x Sex	F (3, 99) = 3.083	0.0308
	Week x Treatment	F (3, 99) = 0.3734	0.7724
	Sex x Treatment	F (1, 33) = 4.145	0.0498
	Week x Sex x Treatment	F (3, 99) = 2.443	0.0686
Body weight – experiment 1 (Fig 1C) Post-hoc within males 2-way (Week, Treatment) ANOVA	Week	F (1.597, 23.95) = 62.79	<0.0001
	Treatment	F (1, 15) = 1.070	0.3172
	Week x Treatment	F (3, 45) = 0.9191	0.4393
Body weight – experiment 1 (Fig 1C) Post-hoc within females 2-way (Week, Treatment) ANOVA	Week	F (2.386, 42.96) = 300.1	<0.0001
	Treatment	F (1, 18) = 4.520	0.0476
	Week x Treatment	F (3, 54) = 3.188	0.0309
Ado DID EtOH – experiment 2 (Fig 1E) 2-way (Day, Sex) ANOVA	Day	F (7.433, 128.8) = 11.26	<0.0001
	Sex	F (1, 18) = 0.1146	0.7389
	Day x Sex	F (15, 260) = 0.5982	0.8754
Body weight – experiment 2 (Fig 1F) 3-way (Week, Sex, Treatment) ANOVA	Week	F (2.100, 75.58) = 289.8	<0.0001
	Sex	F (1, 36) = 42.17	<0.0001
	Treatment	F (1, 36) = 0.2492	0.6207
	Week x Sex	F (3, 108) = 3.765	0.0129
	Week x Treatment	F (3, 108) = 0.4191	0.7396
	Sex x Treatment	F (1, 36) = 0.002849	0.9577
	Week x Sex x Treatment	F (3, 108) = 1.094	0.3549
Ado DID EtOH – experiment 3 (Fig 1H) 2-way (Day, Sex) ANOVA	Day	F (15, 150) = 10.78	<0.0001
	Sex	F (1, 10) = 0.0008475	0.9773
	Day x Sex	F (15, 145) = 1.231	0.2553
Body weight – experiment 3 (Fig 1I) 3-way (Week, Sex, Treatment) ANOVA	Week	F (1.916, 76.63) = 462.8	<0.0001
	Sex	F (1, 40) = 71.57	<0.0001
	Treatment	F (1, 40) = 1.597	0.2136
	Week x Sex	F (3, 120) = 8.902	<0.0001
	Week x Treatment	F (3, 120) = 0.2274	0.8772
	Sex x Treatment	F (1, 40) = 0.1586	0.6926
	Week x Sex x Treatment	F (3, 120) = 0.3506	0.7888

Supplemental Table 1: All ANOVA outcomes for adolescent DID and body weight data presented in Figure 1 of the main text.

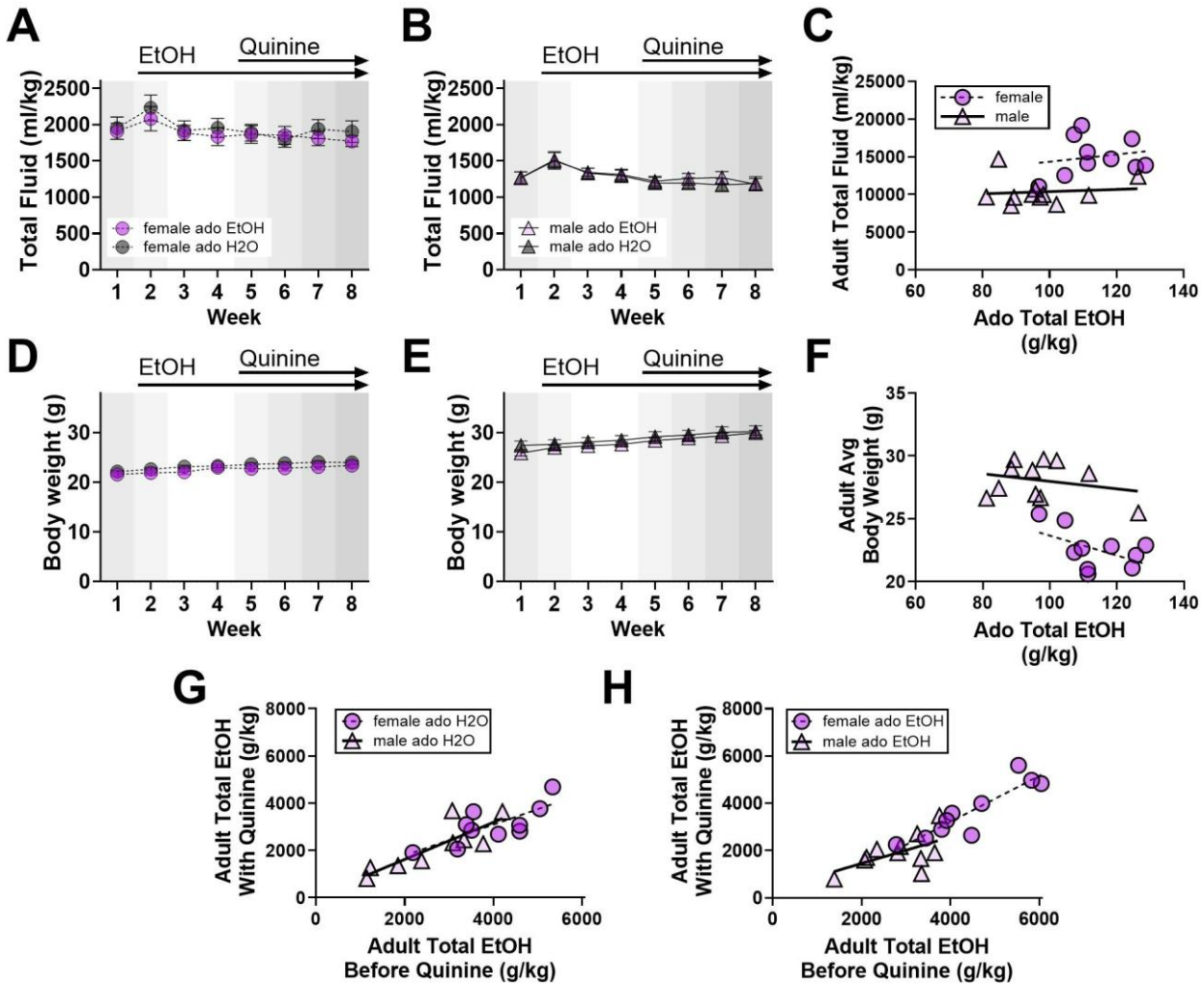

3.2 Adult preference for alcohol and quinine-adulterated alcohol after adolescent drinking

Supp Fig 1. Adolescent alcohol consumption did not affect total fluid consumption (**A-C**) or body weight (**D-F**) during two-bottle choice assessment of alcohol preference. Total alcohol consumed in the first weeks of adult two-bottle choice testing without quinine was significantly associated with total alcohol consumed with quinine (total EtOH no quinine: 0.6538 ± 0.1799, p = 0.0009), but this did not differ across sex or adolescent alcohol treatment groups (**G-H**). Ado = Adolescent. Week 1 represents consumption of H2O only, Week 2 includes 3-7% EtOH, Week 3-4 represents 10% EtOH, and Weeks 5-8 represent 10% EtOH with increasing concentrations of quinine (0.03, 0.1, 0.3, and 1mM). Plots labeled as “Before Quinine” represent data from Weeks 1-4, and plots labeled as “With Quinine” represent data from Weeks 5-8. In scatter plots, a simple linear regression was used to generate lines of best fit and aid interpretation but were independent from statistical analysis. Data are shown as mean +/- SEM. * p <0.05. n=9-11/sex/treatment.

Dependent variable	Effect	F (DFn, DFd)	p
Female EtOH Preference (Fig 2A) 2-way (Week, Treatment) mixed effects ANOVA	Week	F (3.879, 69.82) = 109.1	<0.0001
	Treatment	F (1, 18) = 4.688	0.0441
	Week x Treatment	F (6, 108) = 1.541	0.1717
Female EtOH Consumption (Fig 2B) 2-way (Week, Treatment) mixed effects ANOVA	Week	F (4.501, 81.01) = 99.42	<0.0001
	Treatment	F (1, 18) = 1.530	0.2320
	Week x Treatment	F (6, 108) = 1.562	0.1654
Female H2O Consumption (Fig 2C) 2-way (Week, Treatment) mixed effects ANOVA	Week	F (4.165, 74.97) = 124.5	<0.0001
	Treatment	F (1, 18) = 3.209	0.0900
	Week x Treatment	F (7, 126) = 1.991	0.0613
Female Fluid Consumption (Supp Fig 1A) 2-way (Week, Treatment) mixed effects ANOVA	Week	F (3.979, 71.62) = 4.473	0.0028
	Treatment	F (1, 18) = 0.2025	0.6581
	Week x Treatment	F (7, 126) = 0.5347	0.8068
Female Adult Body Weight (Supp Fig 1D) 2-way (Week, Treatment) mixed effects ANOVA	Week	F (4.113, 74.03) = 40.14	<0.0001
	Treatment	F (1, 18) = 1.690	0.2099
	Week x Treatment	F (7, 126) = 1.471	0.1835
Male EtOH Preference (Fig 2A) 2-way (Week, Treatment) mixed effects ANOVA	Week	F (3.197, 57.54) = 27.01	<0.0001
	Treatment	F (1, 18) = 0.1918	0.6667
	Week x Treatment	F (6, 108) = 0.9424	0.4680
Male EtOH Consumption (Fig 2B) 2-way (Week, Treatment) mixed effects ANOVA	Week	F (3.240, 58.32) = 43.65	<0.0001
	Treatment	F (1, 18) = 0.01788	0.8951
	Week x Treatment	F (6, 108) = 0.8304	0.5489
Male H2O Consumption (Fig 2C) 2-way (Week, Treatment) mixed effects ANOVA	Week	F (3.796, 68.32) = 39.85	<0.0001
	Treatment	F (1, 18) = 0.1121	0.7417
	Week x Treatment	F (7, 126) = 0.7018	0.6705
Male Fluid Consumption (Supp Fig 1A) 2-way (Week, Treatment) mixed effects ANOVA	Week	F (3.346, 60.23) = 8.415	<0.0001
	Treatment	F (1, 18) = 0.05844	0.8117
	Week x Treatment	F (7, 126) = 0.3125	0.9472
Male Adult Body Weight (Supp Fig 1D) 2-way (Week, Treatment) mixed effects ANOVA	Week	F (1.919, 34.55) = 41.94	<0.0001
	Treatment	F (1, 18) = 0.5886	0.4529
	Week x Treatment	F (7, 126) = 1.018	0.4216

Supplemental Table 2: All ANOVA outcomes for experiment 1 examining adolescent DID effects on adult alcohol preference (presented in main text Figure 2 and Supplemental Figure 1).

Dependent variable	Distribution, Link	Effect	Estimate	SE	p	Coefficient Lower	Coefficient Upper
Adult Average EtOH Preference Before Quinine (Fig 2G)	Normal, Identity	Sex (Male)	-1.22	0.51557	0.03011	-2.3077	-0.1322
		Ado EtOH	-0.0092989	0.0040242	0.033658	-0.017789	-0.00080853
		Sex x Ado EtOH	0.0098572	0.0047175	0.052005	-9.5843e-05	0.01981
Adult Total EtOH (g/kg) Before Quinine (Fig 2H)	Normal, Identity	Sex (Male)	-7300.1	2334.3	0.006135	-12225	-2375.1
		Ado EtOH	-77.03	19.392	0.00098475	-117.94	-36.116
		Sex x Ado EtOH	46.756	21.202	0.04149	2.0245	91.488
Post-hoc Female Adult Total EtOH	Normal, Identity	Ado EtOH	5.493	2.7744	0.063213	-0.33576	11.322

(g/kg) Before Quinine (Fig 2I)							
Post-hoc Male Adult Total EtOH (g/kg) Before Quinine (Fig 2I)	Normal, Identity	Ado EtOH	1.9742	3.0892	0.53084	-4.5161	8.4644
Adult Total H2O (ml/kg) Before Quinine (Fig 2I)	Normal, Identity	Sex (Male)	4185.9	3304.3	0.22231	-2785.6	11157
		Ado EtOH	41.761	24.241	0.10308	-9.3835	92.906
		Sex x Ado EtOH	-42.641	30.437	0.17922	-106.86	21.576
Adult Average EtOH Preference After Quinine (Fig 2J)	Normal, Identity	Sex (Male)	-1.1404	0.55206	0.054451	-2.3051	0.024371
		Ado EtOH	-0.010501	0.0043085	0.02608	-0.019591	-0.0014108
		Sex x Ado EtOH	0.0090691	0.0050514	0.090393	-0.0015884	0.019727
Adult Total EtOH (g/kg) After Quinine (Fig 2K)	Normal, Identity	Sex (Male)	-7122.3	2759.8	0.019438	-12945	-1299.7
		Ado EtOH	-85.924	22.866	0.0015686	-134.17	-37.68
		Sex x Ado EtOH	45.618	25.074	0.086519	-7.2836	98.52
Adult Total H2O (ml/kg) After Quinine (Fig 2L)	Normal, Identity	Sex (Male)	6981.3	3163.4	0.041357	307.19	13655
		Ado EtOH	73.618	23.207	0.005571	24.655	122.58
		Sex x Ado EtOH	-65.655	29.139	0.037746	-127.13	-4.1768
Post-hoc Female Adult Total H2O (ml/kg) After Quinine (Fig 2L)	Normal, Identity	Ado EtOH	-6.1345	3.6053	0.10606	-13.709	1.44
Post-hoc Male Adult Total H2O (ml/kg) After Quinine (Fig 2L)	Normal, Identity	Ado EtOH	4.9504	5.0169	0.33685	-5.5898	15.491
Adult Total Fluid (ml/kg) (Supp Fig 1C)	Normal, Identity	Sex (Male)	-1030	8088.2	0.90016	-18095	16035
		Ado EtOH	-1.8252	64.541	0.97777	-137.99	134.34
		Sex x Ado EtOH	-32.213	73.819	0.66806	-187.96	123.53
Adult Average Body Weight (g) (Supp Fig 1F)	Normal, Identity	Sex (Male)	-1.5712	5.7126	0.7866	-13.624	10.481
		Ado EtOH	-0.080137	0.043694	0.084215	-0.17232	0.01205
		Sex x Ado EtOH	0.058422	0.052389	0.2803	-0.05211	0.16895
Adult Total EtOH (g/kg) After Quinine (Supp Fig 1G-H)	Normal, Identity	Sex (Male)	-430.45	874.5	0.62593	-2211.8	1350.9
		Adult EtOH Before Quinine	0.65376	0.17992	0.00096826	0.28727	1.0202
		Ado EtOH group	-1153.3	1037.1	0.27444	-3265.8	959.32
		Sex x Adult EtOH Before Quinine	0.1325	0.24655	0.5947	-0.36971	0.63471
		Sex x Ado EtOH Group	1451	1308.4	0.27571	-1214.2	4116.2
		Adult EtOH Before Quinine x Ado EtOH Group	0.31943	0.24175	0.19576	-0.17299	0.81185
		Sex x Adult EtOH Before Quinine x Ado EtOH Group	-0.54941	0.36712	0.14431	-1.2972	0.19838

Supplemental Table 3: All GLME outcomes for experiment 1 examining adolescent DID effects on adult alcohol preference (presented in main text Figure 2 and Supplemental Figure 1).

Dependent variable	Effect	F (DFn, DFd)	p
OFT Latency to Enter Center (Fig 3A) 2-way (Sex, Treatment) ANOVA	Sex	F (1, 35) = 2.239e-007	0.9996
	Treatment	F (1, 35) = 0.03709	0.8484
	Sex x Treatment	F (1, 35) = 0.5840	0.4499
OFT Time in Center (Fig 3B) 2-way (Sex, Treatment) ANOVA	Sex	F (1, 35) = 3.126	0.0858
	Treatment	F (1, 35) = 0.09244	0.7629
	Sex x Treatment	F (1, 35) = 0.02525	0.8747
OFT Distance Traveled (Fig 3C) 2-way (Sex, Treatment) ANOVA	Sex	F (1, 35) = 0.3328	0.5677
	Treatment	F (1, 35) = 3.918	0.0557
	Sex x Treatment	F (1, 35) = 0.3545	0.5554
EPM Latency to Enter Open Arm (Fig 3G) 2-way (Sex, Treatment) ANOVA	Sex	F (1, 32) = 1.083	0.3059
	Treatment	F (1, 32) = 1.212	0.2792
	Sex x Treatment	F (1, 32) = 4.369	0.0446
EPM Time in Open Arms (Fig 3H) 2-way (Sex, Treatment) ANOVA	Sex	F (1, 32) = 0.01212	0.9130
	Treatment	F (1, 32) = 0.01757	0.8954
	Sex x Treatment	F (1, 32) = 0.7769	0.3847
EPM Open Arm Entries (Fig 3I) 2-way (Sex, Treatment) ANOVA	Sex	F (1, 32) = 0.1890	0.6667
	Treatment	F (1, 32) = 0.02276	0.8810
	Sex x Treatment	F (1, 32) = 2.572	0.1186
EPM Head Dips (Fig 3M) 2-way (Sex, Treatment) ANOVA	Sex	F (1, 32) = 0.01434	0.9054
	Treatment	F (1, 32) = 0.008887	0.9255
	Sex x Treatment	F (1, 32) = 0.02216	0.8826
EPM Distance Traveled (Fig 3N) 2-way (Sex, Treatment) ANOVA	Sex	F (1, 32) = 0.4477	0.5082
	Treatment	F (1, 32) = 0.1038	0.7495
	Sex x Treatment	F (1, 32) = 0.06153	0.8057

Supplemental Table 4: All ANOVA outcomes for experiment 3 examining adolescent DID effects on adult exploratory behavior (presented in main text Figure 3). Post-hoc t tests following the interaction of sex and treatment detected for latency to enter an open arm of the EPM did not reveal significant differences between alcohol- and water-treatment groups within males ($t=1.493$, $df=7.103$, $p=0.1784$) or females ($t=1.548$, $df=9.423$, $p=0.1546$).

Dependent variable	Distribution, Link	Effect	Estimate	SE	p	Coefficient Lower	Coefficient Upper
OFT Latency to Enter Center (Fig 3D)	Poisson, Log	Sex (Male)	-0.78722	0.94129	0.41529	-2.7827	1.2082
		Ado EtOH	-0.011345	0.0061267	0.082619	-0.024333	0.0016435
		Sex x Ado EtOH	0.0091045	0.0086616	0.082619	-0.0092572	0.027466
OFT Time in Center (Fig 3E)	Normal, Identity	Sex (Male)	-11.867	13.605	0.39597	-40.708	16.974
		Ado EtOH	-0.12627	0.084656	0.15526	-0.30573	0.053192
		Sex x Ado EtOH	0.050401	0.12437	0.69066	-0.21325	0.31406
OFT Distance Traveled (Fig 3F)	Normal, Identity	Sex (Male)	-268.7	1160.8	0.81987	-2729.5	2192.1
		Ado EtOH	4.8045	7.1446	0.51088	-10.341	19.95
		Sex x Ado EtOH	3.5844	10.673	0.74135	-19.041	26.21
EPM Latency to Enter Open Arm (Fig 3J)	Poisson, Log	Sex (Male)	-3.6773	2.8487	0.21628	-9.7491	2.3945
		Ado EtOH	0.046292	0.011457	0.0010677	0.021872	0.070712
		Sex x Ado EtOH	0.021018	0.025064	0.41486	-0.032404	0.07444
EPM Time in Open Arms (Fig 3K)	Normal, Identity	Sex (Male)	-100.69	45.956	0.045874	-199.25	-2.1203
		Ado EtOH	-0.5524	0.28632	0.074214	-1.1665	0.061697
		Sex x Ado EtOH	0.98271	0.42438	0.036258	0.072505	1.8929
Post-hoc Female EPM Time in Open Arms (Fig 3K)	Normal, Identity	Ado EtOH	-0.65443	0.028956	4.912e-07	-0.72528	-0.58358
Post-hoc Male EPM Time in Open Arms (Fig 3K)	Normal, Identity	Ado EtOH	0.43031	0.3931	0.30553	-0.47619	1.3368
EPM Open Arm Entries (Fig 3L)	Normal, Identity	Sex (Male)	-106.73	45.694	0.034904	-204.73	-8.7215
		Ado EtOH	-0.51325	0.28469	0.092978	-1.1238	0.097356
		Sex x Ado EtOH	1.0538	0.42196	0.025593	0.14881	1.9588
Post-hoc Female EPM Open Arm Entries (Fig 3L)	Normal, Identity	Ado EtOH	-0.55347	0.19474	0.029487	-1.03	-0.076954
Post-hoc Male EPM Open Arm Entries (Fig 3L)	Normal, Identity	Ado EtOH	0.54058	0.36688	0.17885	-0.30544	1.3866
EPM Head Dips (Fig 3O)	Normal, Identity	Sex (Male)	-232.09	70.78	0.0054862	-383.9	-80.283
		Ado EtOH	-0.95715	0.44098	0.047661	-1.903	-0.011331
		Sex x Ado EtOH	2.1466	0.65361	0.0054301	0.74475	3.5485
Post-hoc Female EPM Head Dips (Fig 3O)	Normal, Identity	Ado EtOH	-1.0553	0.23463	0.0041145	-1.6294	-0.48116
Post-hoc Male EPM Head Dips (Fig 3O)	Normal, Identity	Ado EtOH	1.1895	0.56323	0.067676	-0.10934	2.4883
EPM Distance Traveled (Fig 3P)	Normal, Identity	Sex (Male)	-1527.4	733.9	0.056256	-3101.5	46.684
		Ado EtOH	-4.1053	4.5725	0.38447	-13.912	5.7018
		Sex x Ado EtOH	13.567	6.7773	0.065063	-0.96843	28.103

Supplemental Table 5: All GLME outcomes for experiment 3 examining adolescent DID effects on adult exploratory behavior (presented in main text Figure 3).

3.3 Exploration in the OFT and EPM after drinking

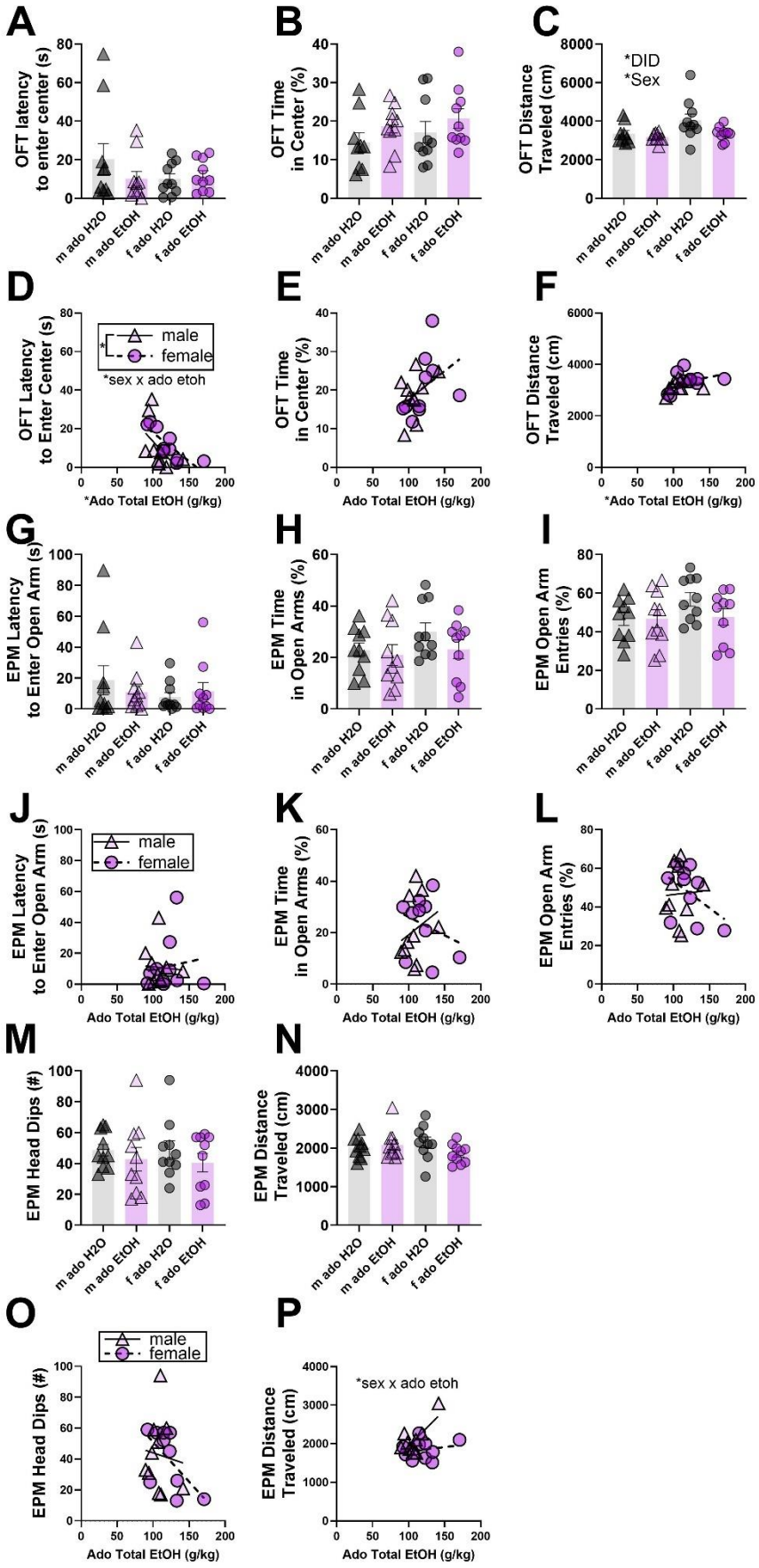

Supp Fig 2. OFT and EPM 24 hrs after adolescent DID. Across DID and sex groups, there were no differences detected in **(A)** OFT latency to enter center of arena or **(B)** OFT percent time spent in center of arena. **(C)** OFT total distance traveled was significantly influenced by DID ($F_{1,35}$ = 4.9, p = 0.0321) and sex ($F_{1,35}$ = 5.0, p = 0.0341). Secondary analyses in only alcohol-exposed subjects found that **(D)** OFT latency to enter center was significantly lower in males than in females (male: -4.5008 ± 1.5347, p = 0.0098), decreased by total alcohol consumed (ado EtOH: -0.03576 ± 0.0082, p = 0.0005), and influenced by a sex by total alcohol interaction (male x ado EtOH: 0.03393 ± 0.01395, p = 0.0271). Post hoc follow-up analyses within sex groups revealed that total alcohol consumption significantly decreased OFT latency to enter the center in females (ado EtOH: -0.2946 ± 0.0658, p = 0.0021) but not in males. **(E)** OFT percent time in center was not associated with adolescent EtOH consumption. **(F)** OFT total distance traveled was significantly increased by total adolescent EtOH consumption (ado EtOH: 8.5896 ± 3.693, p = 0.0335). Across DID and sex groups, there were no differences in **G)** EPM latency to enter an open arm, **(H)** EPM percent time spent in open arms, or **(I)** EPM percent open arm entries. In analyses examining only alcohol-treated subjects, **(J)** EPM latency to enter an open arm, **(K)** EPM percent time spent in open arms, and **(L)** EPM percent open arm entries were not significantly associated with total adolescent EtOH consumption. DID and sex did not influence **M)** EPM number of head dips or **(N)** EPM total distance traveled. In analyses of only alcohol-exposed subjects, **(O)** EPM number of head dips was not associated with total adolescent EtOH consumption. However, **(P)** EPM total distance traveled was influenced by an interaction of total adolescent EtOH consumption and sex (male x ado EtOH: 16.718 ± 6.5302, p = 0.0210). Post hoc follow-up analyses within sex groups revealed that EPM total distance traveled was significantly increased by total adolescent alcohol consumption in males (ado EtOH: 18.88 ± 5.726, p = 0.0110) but not in females. M = male; f = female; ado = adolescent. In scatter plots, a simple linear regression was used to generate lines of best fit and aid interpretation but were independent from statistical analysis. Data are shown as mean +/- SEM. *p<0.05. n=9-10/sex/treatment.

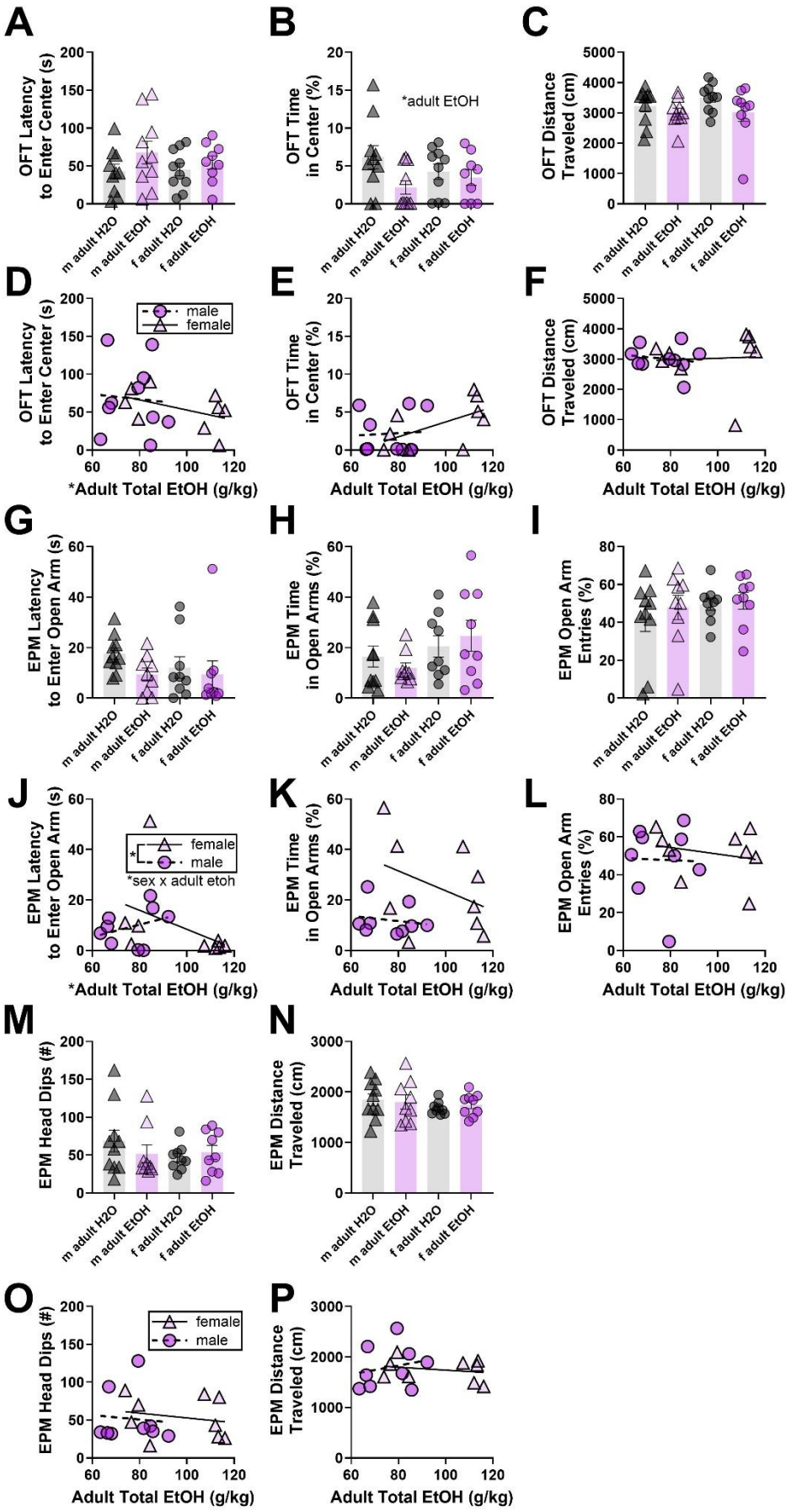
A
OFT Latency to Enter Center (s)
m adult H2O
m adult EtOH
f adult H2O
f adult EtOH
B
OFT Time in Center (%)
*adult EtOH
C
OFT Distance Traveled (cm)
D
male
female
*Adult Total EtOH (g/kg)
E
Adult Total EtOH (g/kg)
F
G
EPM Latency to Enter Open Arm (s)
H
EPM Time in Open Arms (%)
I
EPM Open Arm Entries (%)
J
female
male
*sex x adult etoh
K
L
M
EPM Head Dips (#)
N
EPM Distance Traveled (cm)
O
P

Supp Fig 3. OFT and EPM 30 days after adult DID. Across DID and sex groups, there were no differences found for **A)** OFT latency to enter center of arena. However, **(B)** OFT percent time spent in center of arena was significantly lowered after adult DID ($F_{1,35} = 4.3$, $p = 0.0450$). **(C)** DID and sex did not influence OFT total distance traveled. In separate analyses testing effects of total alcohol consumed among only alcohol-exposed mice, **(D)** OFT latency to enter center was decreased by total alcohol consumed (adult EtOH: -0.0122 ± 0.0026, p = 0.0003). Total alcohol consumed did not significantly alter **(E)** OFT percent time in center or **(F)** OFT total distance traveled compared to adult EtOH consumption. DID and sex did not influence **G)** EPM latency to enter an open arm, **(H)** EPM percent time spent in open arms, or **(I)** EPM percent open arm entries. Analyses within alcohol-treated groups revealed that **(J)** EPM latency to enter an open arm was significantly lower in males than in females (male: -3.2651 ± 1.1546, p = 0.0134), decreased by total alcohol consumed (adult EtOH: -0.0339 ± 0.0081, p = 0.0009), and influenced by a sex by total alcohol interaction (male x adult EtOH: 0.0370 ± 0.0140, p = 0.0193). Follow-up post hoc comparisons within sex groups found that total adult alcohol consumption significantly decreased EPM latency to enter an open arm in females (adult EtOH: -0.0354 ± 0.0082, p = 0.0035) but not in males. Total adult alcohol consumption was not predictive of **(K)** EPM percent time spent in open arms and **(L)** EPM percent open arm entries. Across DID and sex groups, differences were not found in **M)** EPM number of head dips or **(N)** EPM total distance traveled. Total adult alcohol consumption was not associated with **(O)** EPM number of head dips or **(P)** EPM total distance traveled. M = male; f = female. In scatter plots, a simple linear regression was used to generate lines of best fit and aid interpretation but were independent from statistical analysis. Data are shown as mean +/- SEM. *p<0.05. n=9-10/sex/treatment.

3.4 Adolescent binge drinking led to sex-specific alterations in adult whole-brain functional connectivity and pathway-specific connectivity

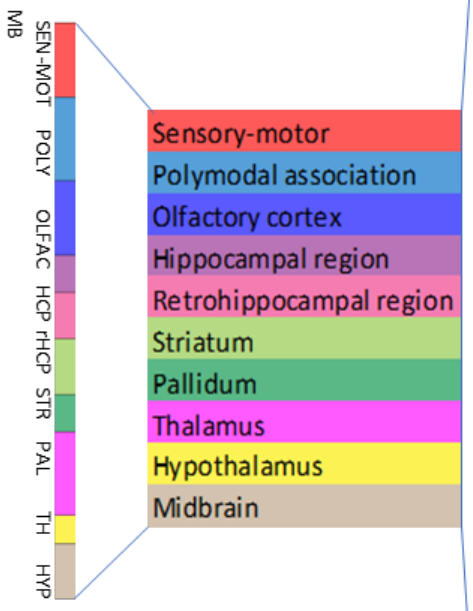

ID	Region	Region Abbv	System name	System ID
1	Gustatory areas	GU	Sensory-motor	1
2	Visceral area	VISC	Sensory-motor	1
3	Primary motor area	MOp	Sensory-motor	1
4	Secondary motor area	MOs	Sensory-motor	1
5	Primary somatosensory area	SSp	Sensory-motor	1
6	Supplemental somatosensory area	SSs	Sensory-motor	1
7	Auditory areas	AUD	Sensory-motor	1
8	visual cortex	VIS	Sensory-motor	1
9	Anterior cingulate area	ACA	Polymodal association	2
10	Prelimbic area	PL	Polymodal association	2
11	Infralimbic area	ILA	Polymodal association	2
12	Orbital area	ORB	Polymodal association	2
13	Agranular insular area	AI	Polymodal association	2
14	Retrosplenial area	RSP	Polymodal association	2
15	Parietal association areas	PTL	Polymodal association	2
16	Temporal association areas	Tev	Polymodal association	2
17	Ectorhinal area	ECT	Polymodal association	2
18	Main olfactory bulb	MOB	Olfactory cortex	3
19	Accessory olfactory bulb	AOB	Olfactory cortex	3
20	Anterior olfactory nucleus	AON	Olfactory cortex	3
21	Taenia tecta	TT	Olfactory cortex	3
22	Piriform area	PIR	Olfactory cortex	3
23	Nucleus of the lateral olfactory tract	NLOT	Olfactory cortex	3
24	Cortical amygdalar area	COA	Olfactory cortex	3
25	Postpiriform transition area	TR	Olfactory cortex	3
26	Dentate gyrus	DG	Hippocampal region	4
27	Field CA1	CA1	Hippocampal region	4
28	Field CA2	CA2	Hippocampal region	4
29	Field CA3	CA3	Hippocampal region	4
30	entorhinal area	ENT	Retrohippocampal region	5
31	presubiculum	PRE	Retrohippocampal region	5
32	postsubiculum	POST	Retrohippocampal region	5
33	parasubiculum	PAR	Retrohippocampal region	5
34	subiculum	SUB	Retrohippocampal region	5
35	Lateral septal complex	LSX	Striatum	6
36	Caudoputamen	CP	Striatum	6
37	Nucleus accumbens	ACB	Striatum	6
38	Olfactory tubercle	OT	Striatum	6
39	Fundus of striatum	FS	Striatum	6
40	Striatum-like amygdalar nuclei	sAMY	Striatum	6
41	Medial septal complex	MSC	Pallidum	7
42	Globus pallidus, external segment	GP	Pallidum	7
43	Substantia innominata	SI	Pallidum	7
44	Bed nuclei of the stria terminalis of Pallidum	BST	Pallidum	7
45	anterior hypothalamic nucleus	ATN	Thalamus	8
46	Ventral group of the dorsal thalamus	VENT	Thalamus	8
47	Lateral group of the dorsal thalamus	LAT	Thalamus	8
48	Medial group of the dorsal thalamus	MED	Thalamus	8
49	Midline group of the dorsal thalamus	MTN	Thalamus	8
50	Medial geniculate complex	MG	Thalamus	8
51	Lateral geniculate complex	LG	Thalamus	8
52	Zona incerta	ZI	Thalamus	8
53	Reticular nucleus of the thalamus	RT	Thalamus	8
54	Hypothalamic lateral zone	LZ	Hypothalamus	9
55	Periventricular zone	PVZ	Hypothalamus	9
56	Hypothalamic medial zone	MEZ	Hypothalamus	9
57	Substantia nigra	SN	Midbrain	10
58	Periaqueductal gray	PAG	Midbrain	10
59	Ventral tegmental area	VTA	Midbrain	10
60	Superior colliculus	SC	Midbrain	10
61	Midbrain reticular nucleus	MRN	Midbrain	10
62	RAmb	RAmb	Midbrain	10

Supp Fig 4. Regions of interest (ROIs) and their associated brain systems were defined based on anatomical classifications from the Allen Mouse Brain Atlas (Lein et al., 2007).

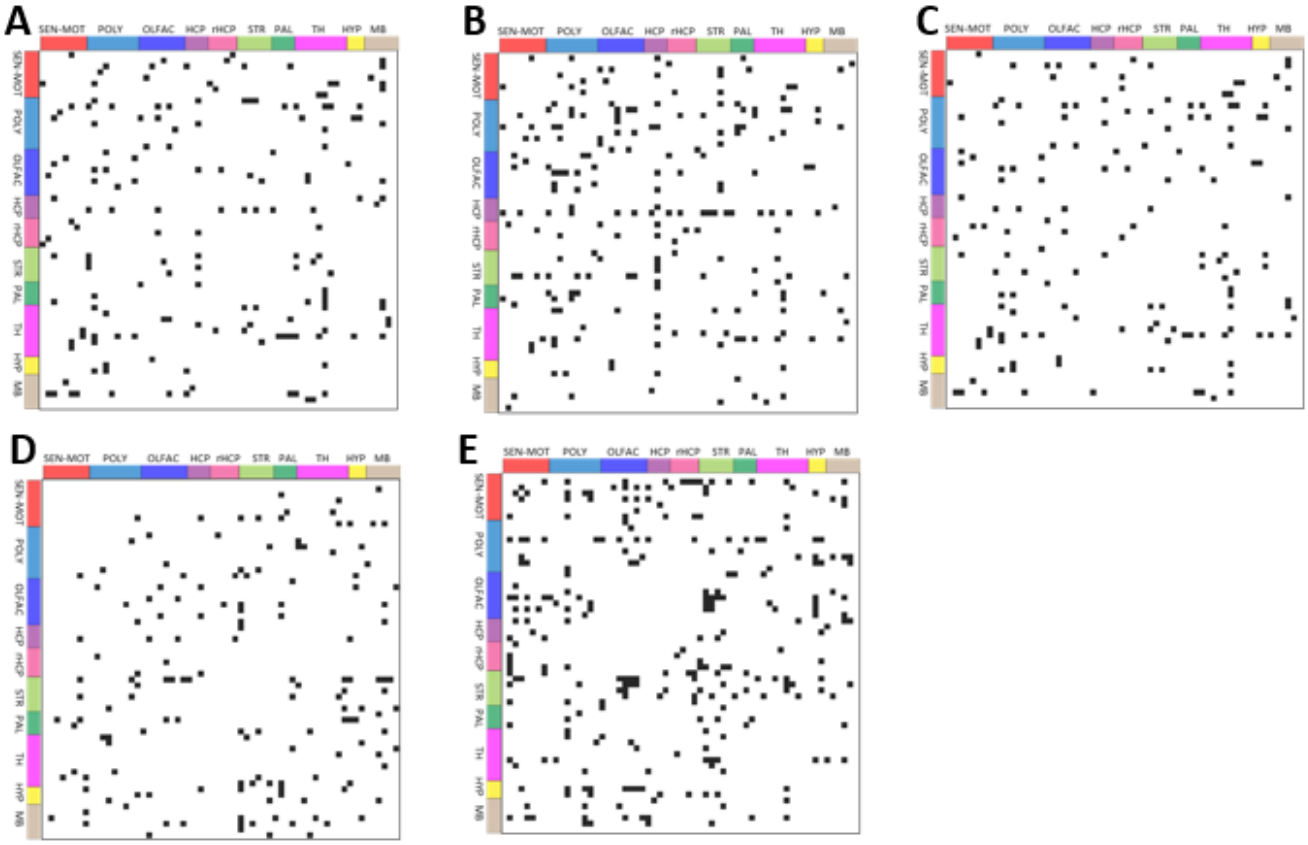

Supp Fig 5. Using linear mixed modeling and a significance threshold of $p<0.05$, pairwise comparisons of RSFC were performed for each ROI. Significant effects of adolescent alcohol group (A), sex (B), and the interaction between adolescent alcohol group and sex (C) were found. (D) Among alcohol-exposed mice, significant effects of total alcohol consumption were found on each pairwise RSFC after accounting for sex. (E) Significant effects of sex were also found on each pairwise RSFC after accounting for total alcohol consumption. The significance threshold was $p<0.05$ (uncorrected) to improve sensitivity for exploratory analysis. n=11 mice/sex/treatment.

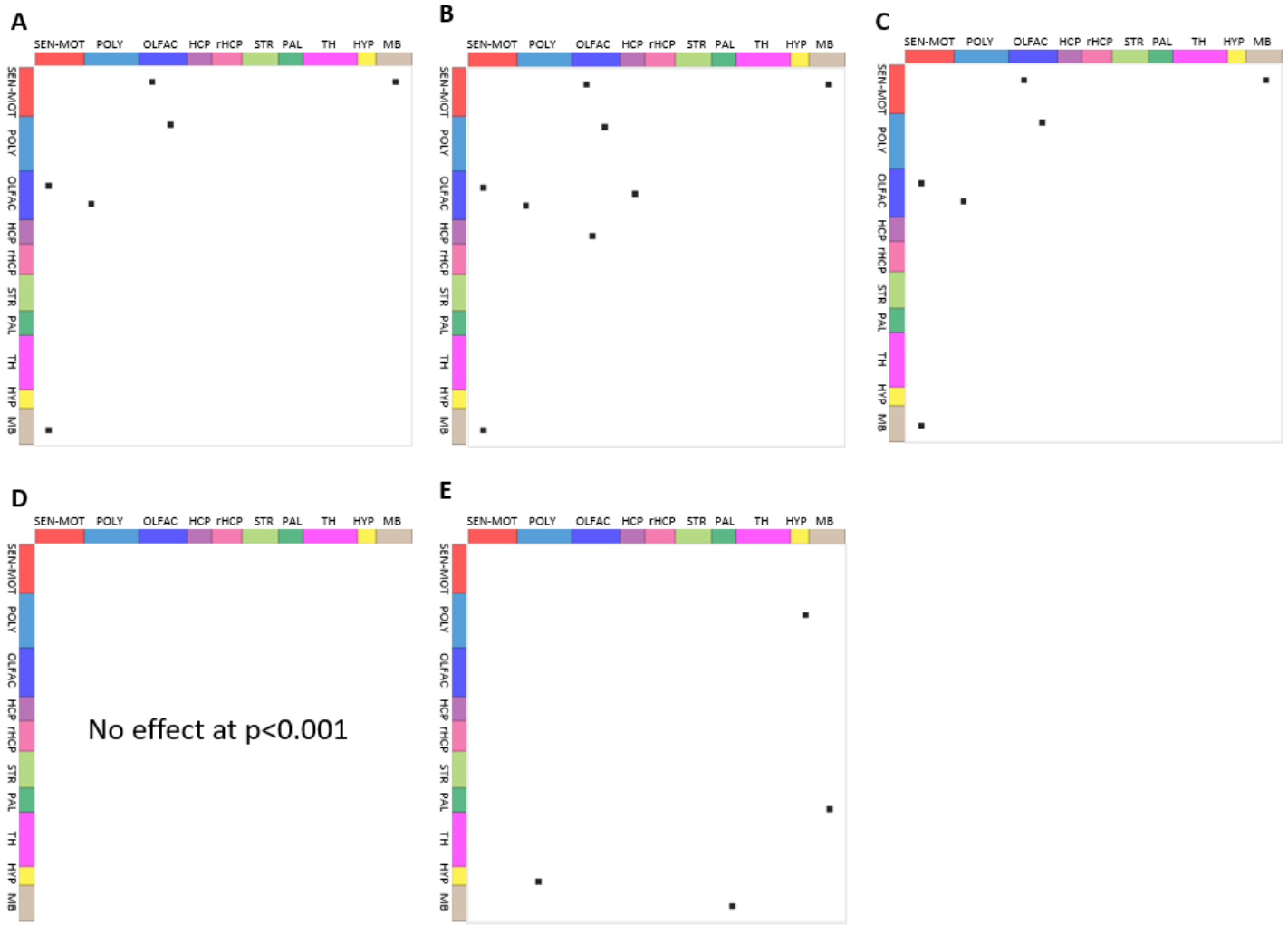

Supp Fig 6. Using linear mixed modeling and a significance threshold of p<0.001, pairwise comparisons of RSFC were performed for each ROI. Effects of adolescent alcohol consumed (A), sex (B), and the interaction between adolescent alcohol and sex (C) were detected. (D) No significant effects of total alcohol consumption were found after accounting for sex. (E) Significant effects of sex were identified after accounting for total alcohol consumption. The significance threshold was p<0.001 to reduce likelihood of Type 1 errors. n=11 mice/sex/treatment.

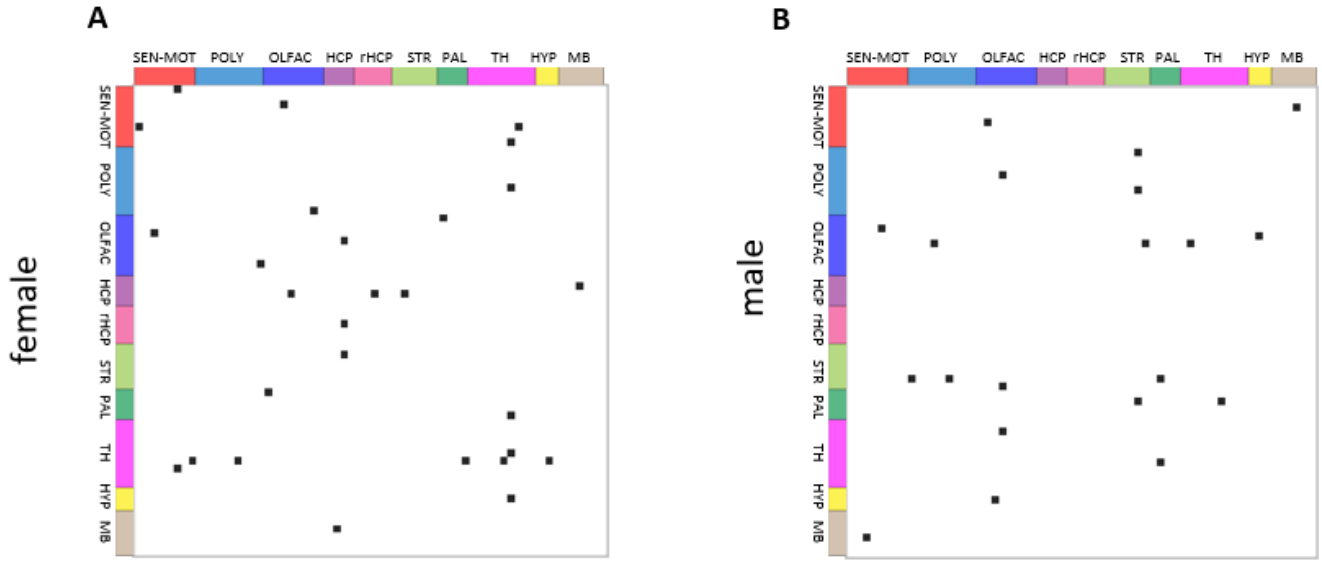

Supp Fig 7. To further explore sex and alcohol interactions, the Tukey's HSD method was used to compare RSFC across alcohol and water groups separately in males and females. n=11 mice/sex/treatment.

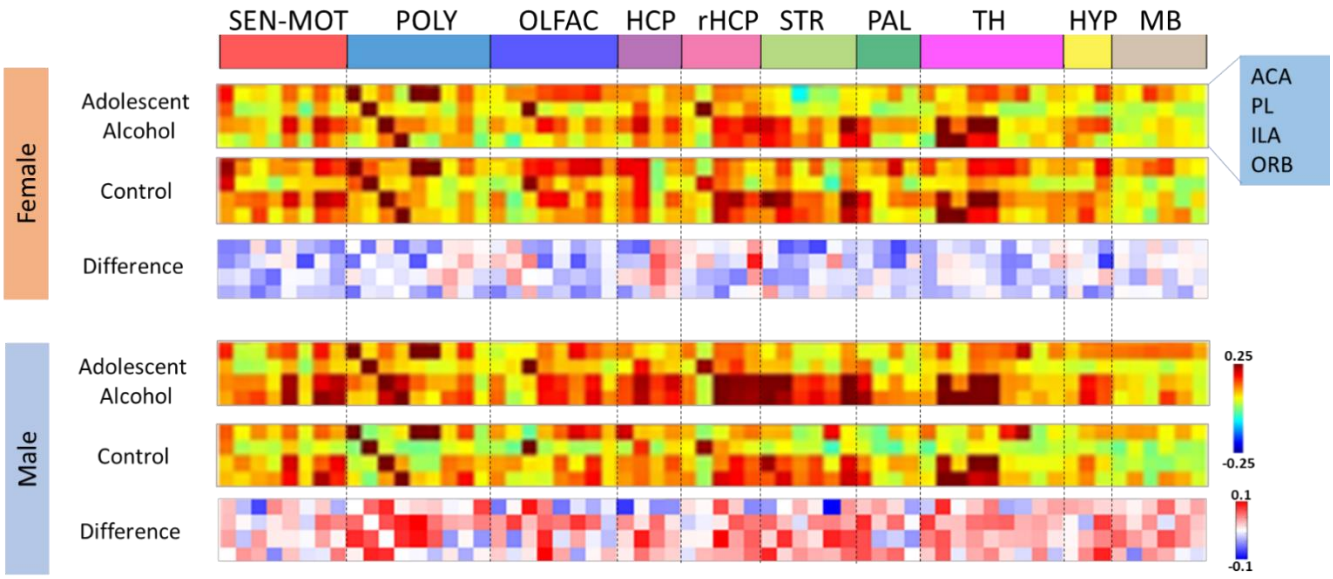

Supp Fig 8. Average functional connectivity patterns of PFC for sex- and treatment-specific groups**,** and sex-specific difference matrices between adolescent alcohol treatment and controls. Each matrix has 4 rows corresponding to the subregions of PFC (ACA: Anterior cingulate area, PL: Prelimbic area, ILA: Infralimbic area, and ORB: Orbital area). In each sex group, the first 2 matrices (1st, 2nd, 4th, and 5th matrices) represent the average RSFC patterns of the subregions of PFC. The color bar (with ± 0.25 range) represents the z-score values for the corresponding RSFC. The third matrices (3rd and 6th matrices) in each sex group show the difference of RSFC between alcohol-treated and control groups in their corresponding sex groups. The red-blue color bar (with ± 0.1 range) shows the z-score differences for the increased or decreased average RSFC in adolescent alcohol-treated mice in comparison to the controls, respectively.

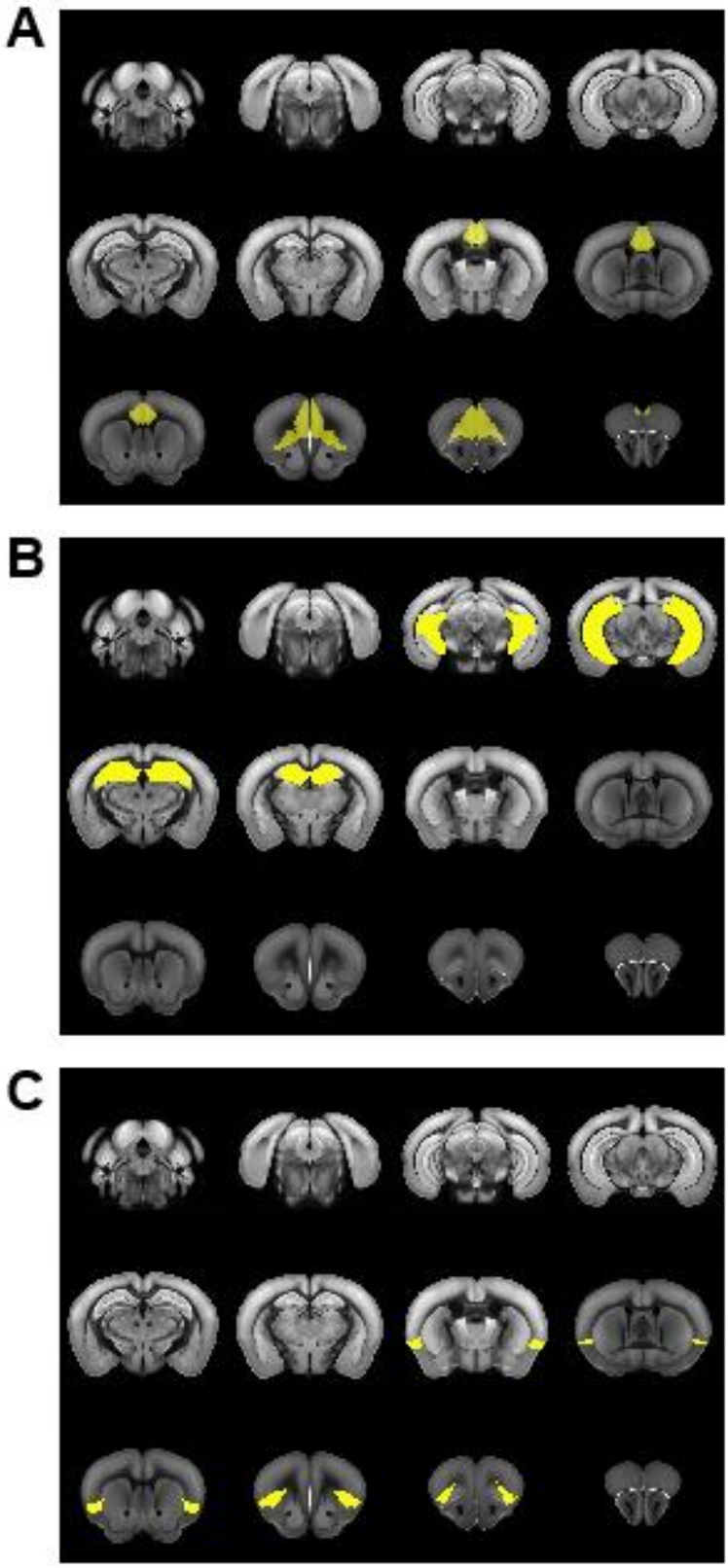

Supp Fig 9. PFC (A), hippocampus (B), and insula (C) seed regions are highlighted in yellow. Seed regions in the mouse brain were defined based on anatomical classifications from the Allen Mouse Brain Atlas (Lein et al., 2007).

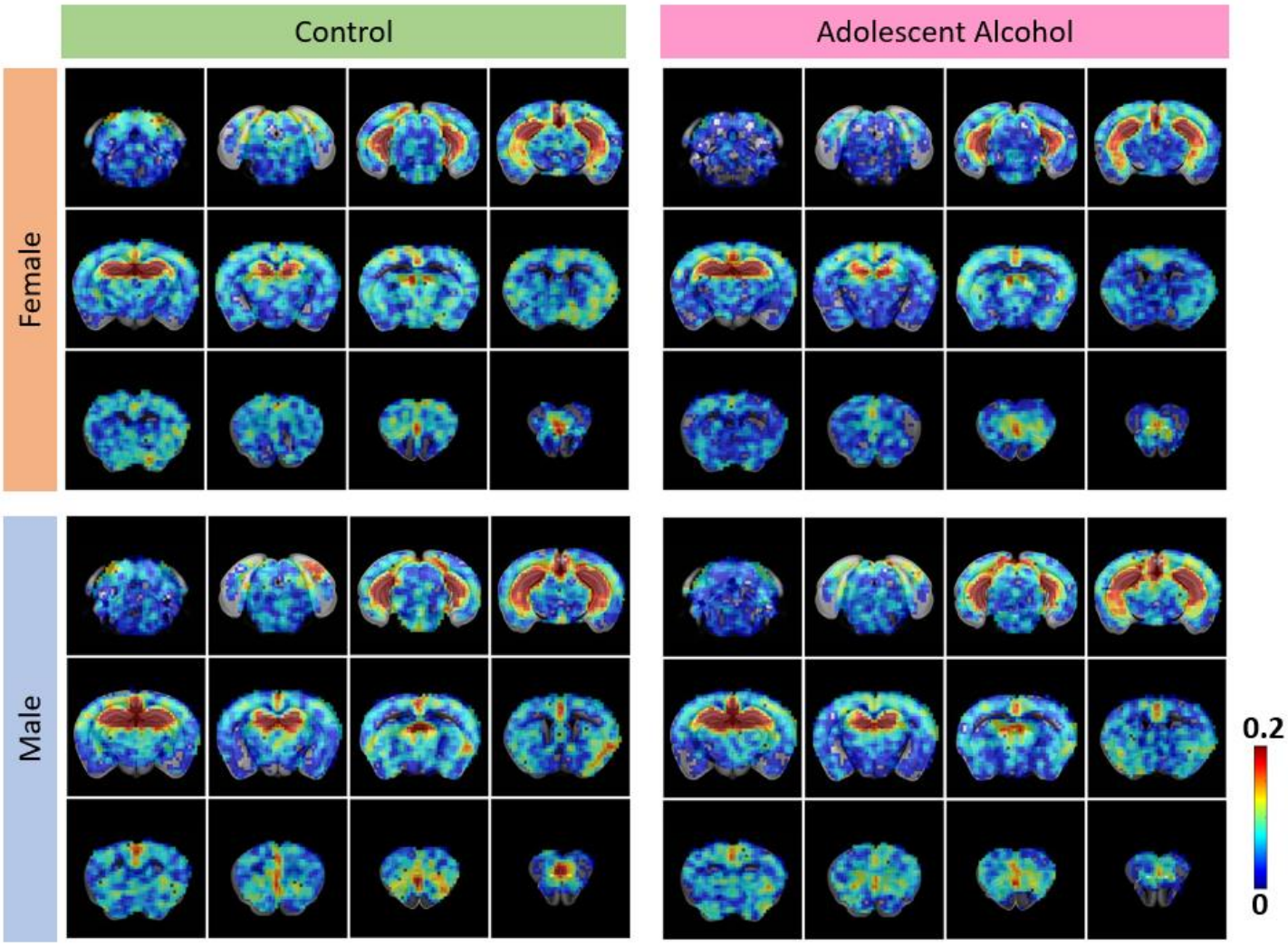

Supp Fig 10. Average seed-based functional connectivity maps of the hippocampus for sex- and treatment-specific groups**.** Anatomical classification of the hippocampus is available in Supp Fig 9. The color bar (± 0.2 range) represents the average correlation values for the corresponding RSFC between the hippocampus and all other voxels. n=11 mice/sex/treatment.

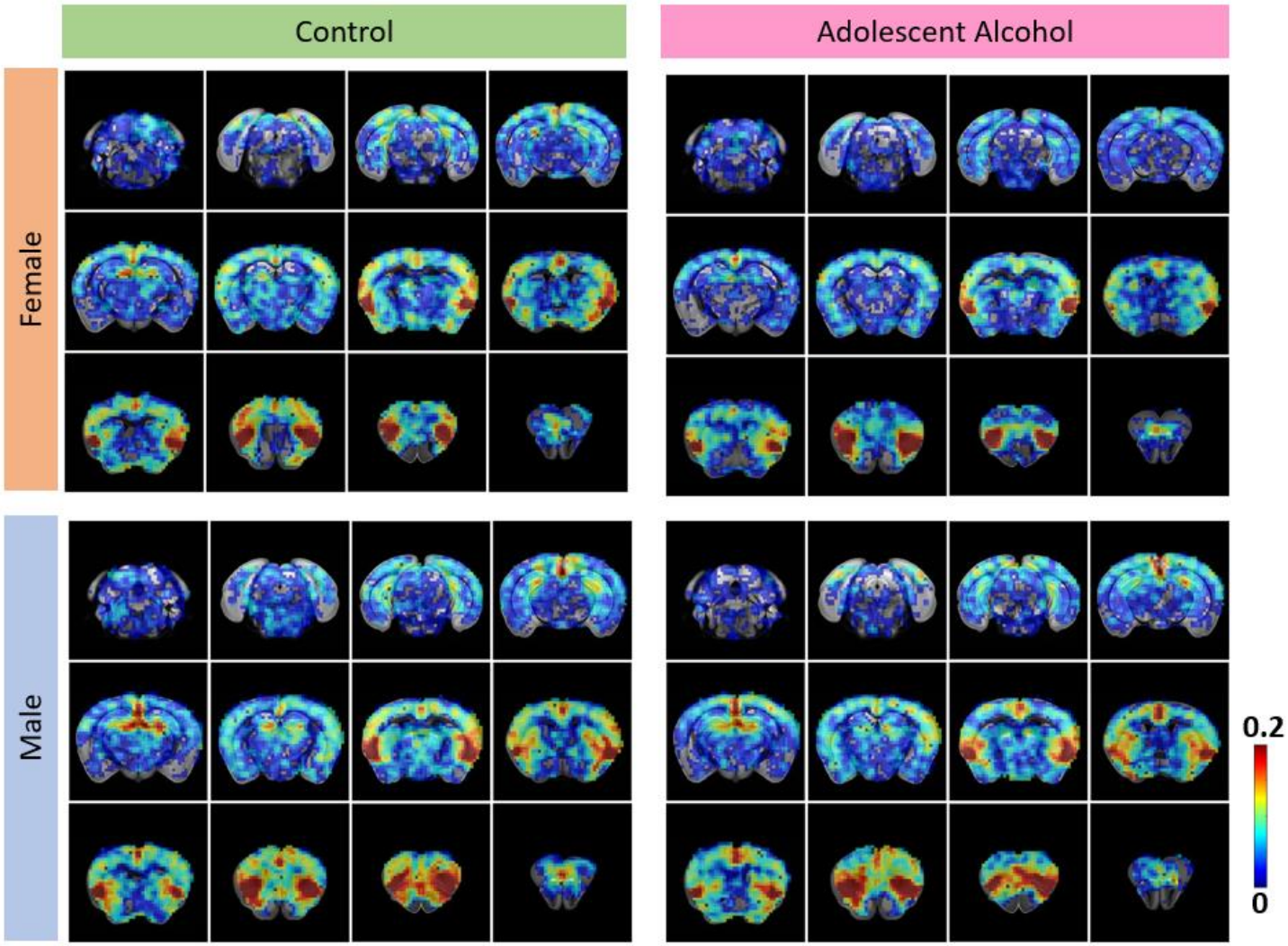

Supp Fig 11. Average seed-based functional connectivity maps of the insula for sex- and treatment-specific groups**.** Anatomical classification of the insula is available in Supp Fig 9. The color bar (± 0.2 range) represents the average correlation values for the corresponding RSFC between the insula and all other voxels. n=11 mice/sex/treatment.

Supp Table 6. Significant associations between total alcohol consumed and RSFC (as displayed in Supp Fig 5D).

ROI 1	ROI 2	Estimate
		positive relationships
Auditory areas	Ectorhinal area	0.003
Infralimbic area	anterior hypothalamic nucleus	0.003
Orbital area	Striatum-like amygdalar nuclei	0.002
Orbital area	anterior hypothalamic nucleus	0.002
Orbital area	Ventral group of the dorsal thalamus	0.002
Orbital area	Hypothalamic medial zone	0.002
Parietal association areas	Piriform area	0.002
Parietal association areas	Substantia nigra	0.003
Ectorhinal area	Postpiriform transition area	0.002
Ectorhinal area	subiculum	0.003
Ectorhinal area	Caudoputamen	0.004
Ectorhinal area	Periventricular zone	0.004
Main olfactory bulb	Bed nuclei of the stria terminalis of Pallidum	0.003
Accessory olfactory bulb	Field CA2	0.004
Accessory olfactory bulb	Periventricular zone	0.003
Accessory olfactory bulb	RAmb	0.003
Caudoputamen	anterior hypothalamic nucleus	0.003
Striatum-like amygdalar nuclei	Hypothalamic medial zone	0.003
Ventral group of the dorsal thalamus	Hypothalamic medial zone	0.003
		negative relationships
Visceral area	Ventral tegmental area	-0.003
Primary motor area	Globus pallidus, external segment	-0.002
Secondary motor area	Zona incerta	-0.003
Supplemental somatosensory area	Substantia innominata	-0.003
Supplemental somatosensory area	Lateral geniculate complex	-0.002
Auditory areas	Field CA2	-0.003
Auditory areas	Lateral septal complex	-0.004
Auditory areas	Olfactory tubercle	-0.004
Auditory areas	Globus pallidus, external segment	-0.002
visual cortex	Zona incerta	-0.003
visual cortex	Hypothalamic lateral zone	-0.003
visual cortex	Periaqueductal gray	-0.003
visual cortex	Superior colliculus	-0.003
Prelimbic area	Accessory olfactory bulb	-0.002
Prelimbic area	presubiculum	-0.002
Infralimbic area	Temporal association areas	-0.003
Agranular insular area	Lateral geniculate complex	-0.003
Temporal association areas	Lateral septal complex	-0.003
Temporal association areas	Olfactory tubercle	-0.004

Accessory olfactory bulb	Taenia tecta	-0.004
Taenia tecta	Cortical amygdalar area	-0.003
Piriform area	postsubiculum	-0.003
Piriform area	Lateral septal complex	-0.004
Piriform area	Globus pallidus, external segment	-0.003
Piriform area	Superior colliculus	-0.003
Nucleus of the lateral olfactory tract	Lateral septal complex	-0.004
Cortical amygdalar area	Field CA2	-0.003
Cortical amygdalar area	Globus pallidus, external segment	-0.002
Postpiriform transition area	Lateral septal complex	-0.003
Postpiriform transition area	Superior colliculus	-0.002
Dentate gyrus	Lateral septal complex	-0.004
Field CA2	subiculum	-0.003
Field CA2	Hypothalamic lateral zone	-0.003
Lateral septal complex	Bed nuclei of the stria terminalis of Pallidum	-0.004
Lateral septal complex	Reticular nucleus of the thalamus	-0.003
Lateral septal complex	Hypothalamic lateral zone	-0.003
Lateral septal complex	Ventral tegmental area	-0.002
Lateral septal complex	Superior colliculus	-0.004
Lateral septal complex	Midbrain reticular nucleus	-0.002
Nucleus accumbens	Reticular nucleus of the thalamus	-0.002
Nucleus accumbens	Superior colliculus	-0.004
Olfactory tubercle	Bed nuclei of the stria terminalis of Pallidum	-0.003
Olfactory tubercle	Zona incerta	-0.002
Striatum-like amygdalar nuclei	Reticular nucleus of the thalamus	-0.002
Striatum-like amygdalar nuclei	RAmb	-0.002
Medial septal complex	Ventral tegmental area	-0.002
Globus pallidus, external segment	Reticular nucleus of the thalamus	-0.003
Globus pallidus, external segment	Hypothalamic lateral zone	-0.002
Globus pallidus, external segment	Periventricular zone	-0.003
Bed nuclei of the stria terminalis of Pallidum	Lateral group of the dorsal thalamus	-0.002
Bed nuclei of the stria terminalis of Pallidum	Superior colliculus	-0.002
Lateral group of the dorsal thalamus	RAmb	-0.003
Medial group of the dorsal thalamus	Zona incerta	-0.003
Medial group of the dorsal thalamus	Ventral tegmental area	-0.002
Medial geniculate complex	Superior colliculus	-0.003
Reticular nucleus of the thalamus	Hypothalamic lateral zone	-0.002
Hypothalamic medial zone	Ventral tegmental area	-0.002